202
3/3/70

1249

AI-AEC-12922
COPY

MASTER

LARGE RADIOISOTOPE HEAT SOURCE CAPSULE PROGRAM

TOPICAL REPORT NO. 8

CAPSULE IMPACT TESTING

AEC Research and Development Report

Atomics International
North American Rockwell

P.O. Box 309
Canoga Park, California 91304

P-3377

DISCLAIMER

Printed in the United States of America
Available from
Clearinghouse for Federal Scientific and Technical Information
National Bureau of Standards, U.S. Department of Commerce
Springfield, Virginia 22151
Price: Printed Copy $3.00; Microfiche $0.65

AI-AEC-12922
PROPULSION SYSTEMS AND
ENERGY CONVERSION

LARGE RADIOISOTOPE HEAT SOURCE CAPSULE PROGRAM

TOPICAL REPORT NO. 8

CAPSULE IMPACT TESTING

By

J. M. HARRIS

This report has been prepared under
Contract AT(29-2)-2338 with the
U.S. Atomic Energy Commission

Atomics International
North American Rockwell

P.O. Box 309
Canoga Park, California 91304

CONTRACT: AT(29-2)-2338
ISSUED: JANUARY 23, 1970

DISTRIBUTION

This report has been distributed according to the category "Propulsion Systems and Energy Conversion," as given in the Standard Distribution for Unclassified Scientific and Technical Reports, TID-4500.

CONTENTS

TABLES

FIGURES

FIGURES

ABSTRACT

The Large Radioisotope Heat Source Capsule (LRHSC) Program is developing the technology for a high temperature (≥2000°F), long life (≥5 years) radioisotope heat source which can be used in the space environment. The program is specifically concerned with the development of a tantalum alloy fuel capsule. Materials compatibility, fabrication processes and assembly procedures are being defined, and the response of the capsule is being determined for conditions of biaxial creep, terminal velocity impact and launch pad abort testing.

This report contains the results of the LRHSC Impact Test Program. This test program was performed to establish the behavior of the refractory metal capsule upon reentry impact. Twelve LRHS capsules were impact tested at various angles at the Atomics International Impact Test Facility. Upon completion of testing a complete post-test analysis was performed on each capsule.

PAGE BLANK

I. INTRODUCTION

Atomics International, a Division of North American Rockwell Corporation, under contract with the Atomic Energy Commission,* has developed the fabrication and assembly techniques required to produce a high temperature, tantalum alloy fuel capsule. As part of this program a series of capsules have been impact tested to determine the behavior of the materials and components during reentry impact.

The Large Radioisotope Heat Source Capsule (LRHSC), depicted in Figure 1, uses tantalum base alloy members for the basic radioisotope fuel containment vessel. Ta-10W liner components position the fuel in a cylindrical annulus with an excluded volume available as a plenum for the helium which is generated by alpha decay of the fuel. The T-111 (Ta-8W-2Hf) structural shell provides the primary containment. The Pt-10Rh clad provides oxidation protection for the tantalum alloys during air exposure. The alumina diffusion barrier between the structural shell and clad prevents interdiffusion of the dissimilar noble and refractory metals. The Pt-10Rh shell is arc plasma sprayed with a high emissivity coating of iron titanate.

The terminal velocity impact tests reported herein were designed to determine the capability of the reference capsule materials to survive reentry impact, to determine the failure modes of the reference capsule design and to ascertain the relative influence of various capsule design parameters on capsule survival. Twelve capsules were impacted at the NR impact test facility described in Section II. The test conditions for each capsule and a summary of the test results are presented in Section III. The details on the post-test analysis of each capsule appear in Section IV. Section V contains an evaluation of the test results in terms of an analytic distribution of impact energies. Section VI presents the conclusions from this test series.

---

*Atomics International Contract Number AT(29-2)-2338

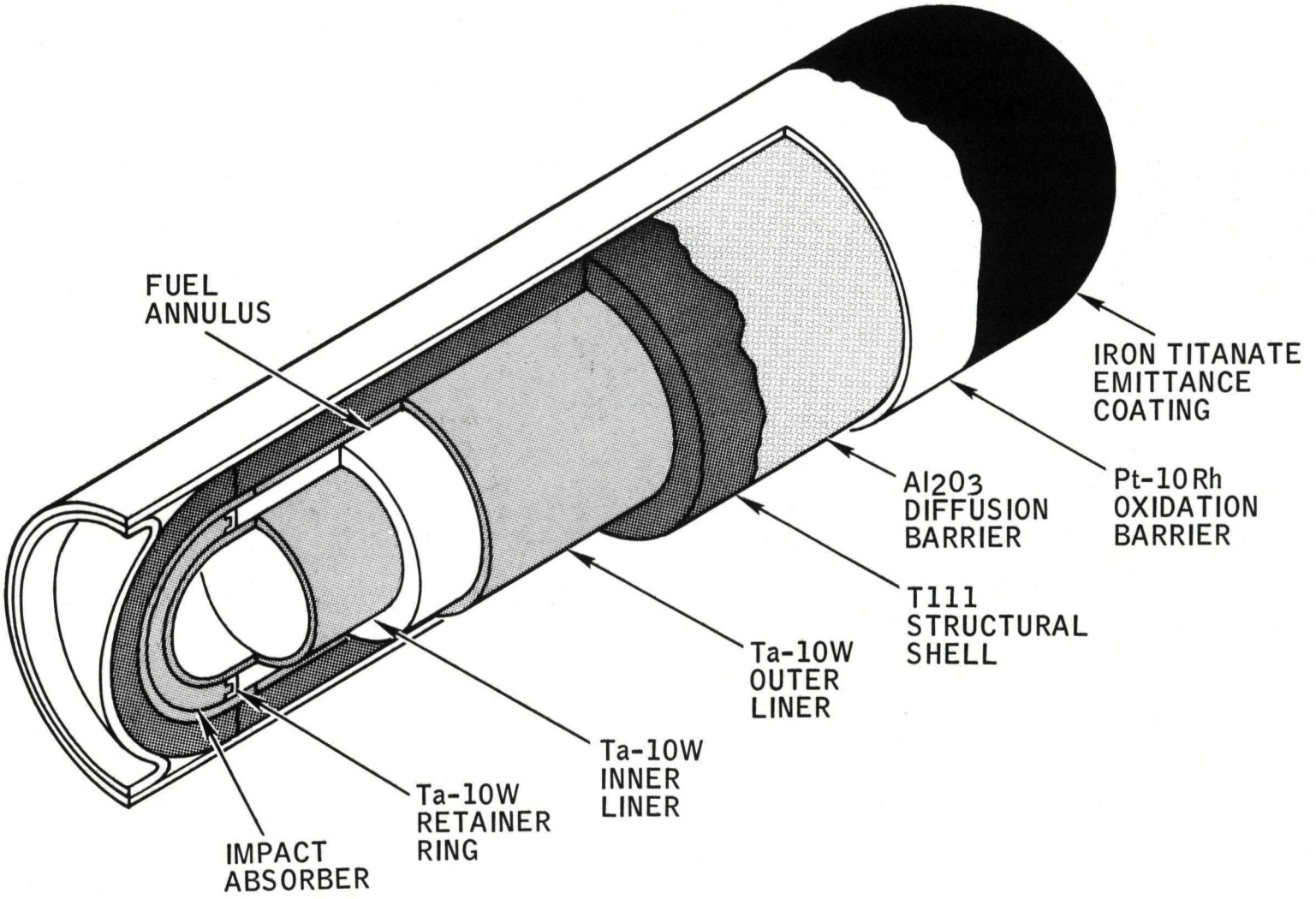

Figure 1. Large Radioisotope Heat Source Capsule (LRHSC)

II. TEST FACILITY AND TESTING PROCEDURES

The NR owned impact facility,[1] Figure 2, was modified to accommodate the LRHSC Impact Program. The modifications included fabricating two impact barrels having the capability of hot breech loading and installing a furnace capable of heating the capsules to 1500°F in an argon atmosphere.

The gas gun shown in Figure 3 is capable of launching various diameter test specimens weighing up to 20 lb at velocities to 1200 fps. A high pressure chamber can be filled with up to 4000 psi N_2 gas. When the gas is exhausted through a 2-in. diameter orifice, by actuating a fast-acting valve, the expanding gas propels the test specimen. Any diameter specimen can be launched with this gun by providing the proper diameter and length barrel. The velocity attained is a function of the specimen weight and diameter, chamber pressure, barrel length, fast-acting valve opening time, and gas used, within the constraints of the gas flow through the 2-in. diameter orifice. The specimen velocity is measured by a set of photocells which activate a microsecond counter to obtain the time of flight between the photocells. The impact target is a 1500-lb block of black granite.

The test procedure for each capsule was as follows. A dummy with a mass and a diameter equal to those of the test capsule was used to calibrate for each test. Using the dummy the air gun chamber pressure for the desired impact velocity was determined. The test capsule was then placed in an argon atmosphere furnace located next to the air gun and brought up to a temperature of 1400°F. The capsule was removed from the furnace with a pair of tongs and dropped into the air gun breech. The breech cover was closed, the immediate area evacuated, and the air gun pressurized and fired. The time from removal of the capsule from the furnace to firing of the gun was 50 to 60 sec. Heat transfer calculations indicate that under these conditions the capsule impact temperature was 1200 ± 25°F. As indicated previously, the actual test velocity was obtained from the microsecond timing device. The air gun firing sequence also activated the high speed cameras for movie coverage of the impact. Analysis of the high speed movies was used as a backup for velocity determination.

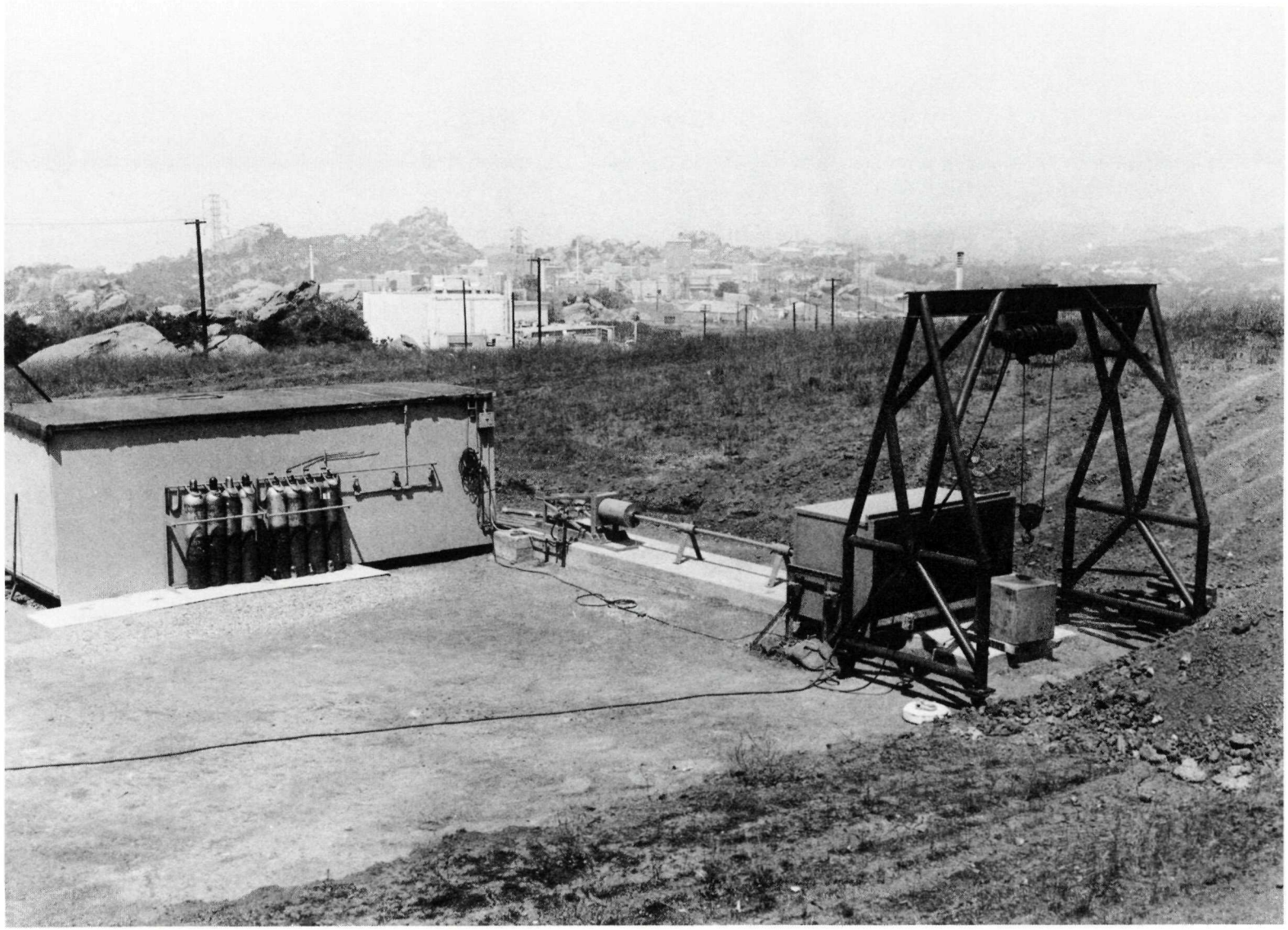

7-18-66

6090-5182CN

Figure 2. NR Impact Facility

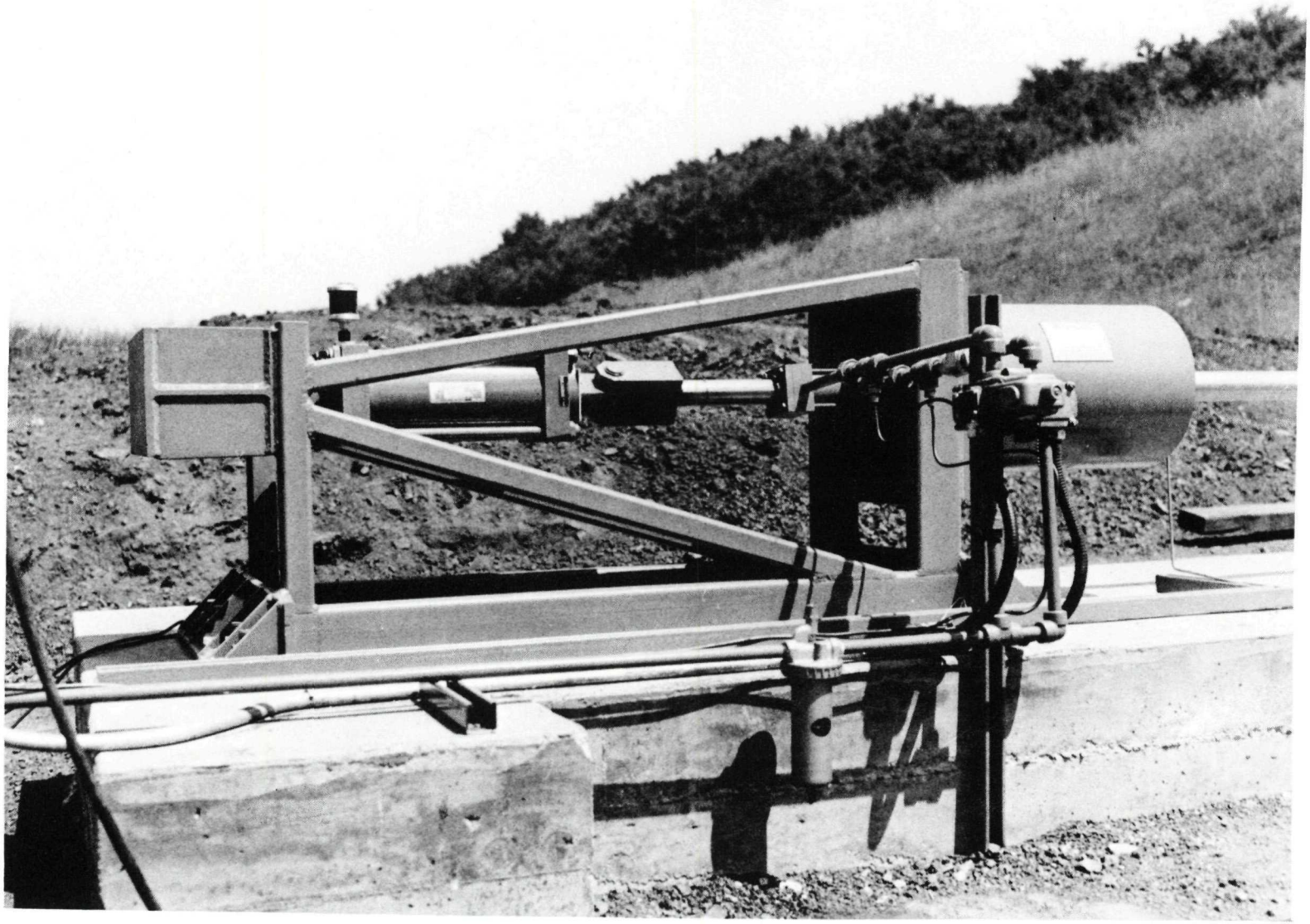

7-18-66

6090-5183CN

Figure 3. Launch Chamber and Fast Opening Valve

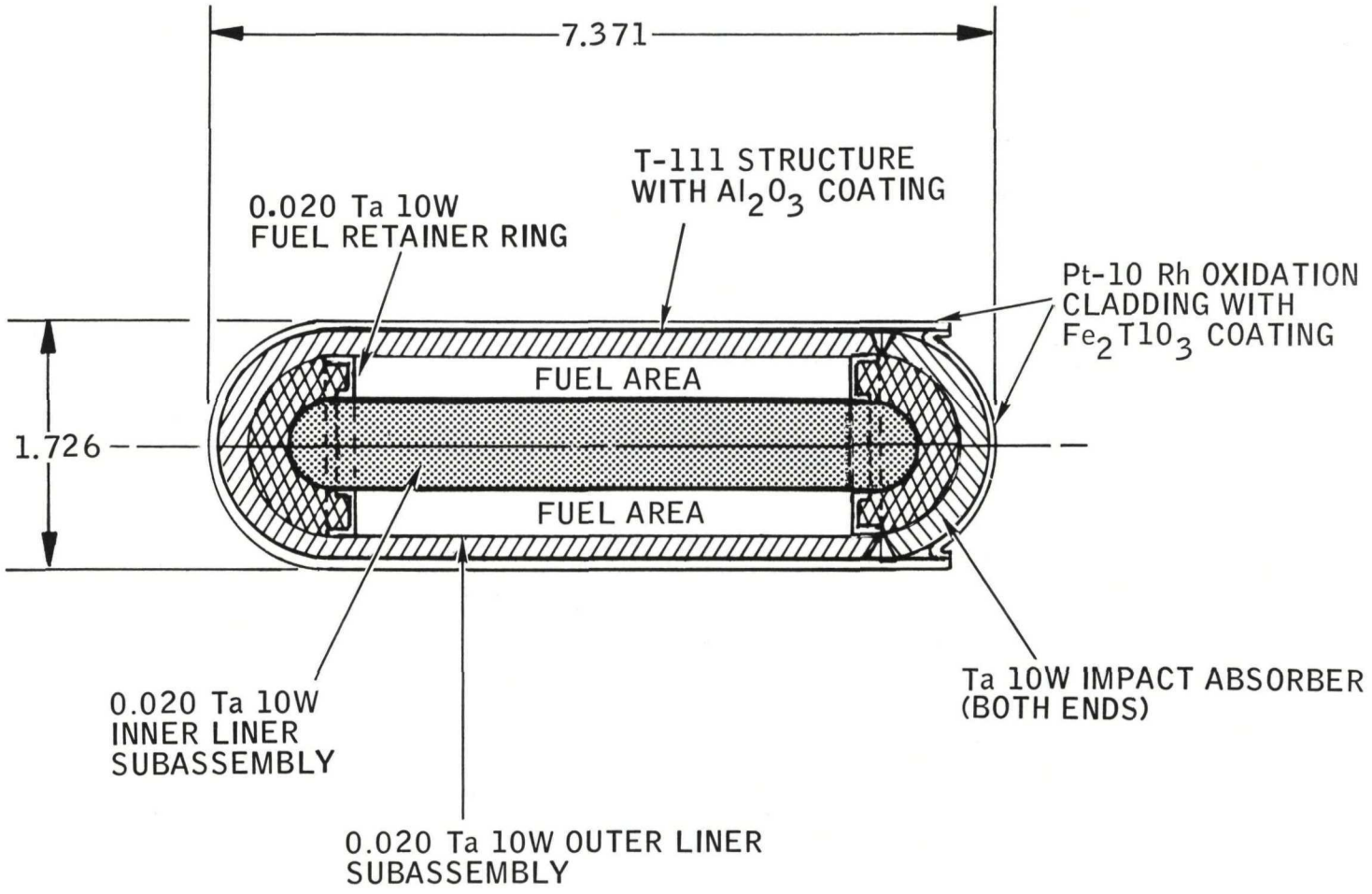

Figure 4. LRHSC Design

III. TEST SERIES SUMMARY

The objective of the LRHSC Impact Test Program was to investigate the capability of the capsule materials and capsule design for surviving terminal velocity impact and to identify the most probable failure mode for the reference capsule. This was accomplished by varying the capsule test parameters. They were varied by changing the impact velocity and the impact angle. The capsule design was varied by changing the capsule wall thickness and by either using or omitting the impact absorber and platinum oxidation barrier. One of the capsules was tested without an inner liner but with solid fuel retainer rings, i.e., it was fully packed with fuel simulant.

The reference 200-watt LRHS capsule design, Figure 4, was utilized in fabricating eleven (A-1 through A-11) impact capsules. Capsule A-24 utilized the liner assembly shown in Figure 5. This design eliminated the inner liner and used fuel retainer discs, thereby increasing the power rating of the capsule to 400 watts.

For all the impact capsules a mixture of tungsten and molybdenum powder was used to simulate the proper mass of a microsphere fuel loading.

The test conditions for each of the capsules in the LRHSC impact test program are shown in Table 1. The twelve impact capsules varied in wall thickness from 0.060 to 0.125 in. and in impact velocity from 230 to 450 ft/sec. The impact temperature was held constant (1200°F) for this series of tests. The impact angle was generally end on but due to the difference between the capsule diameters and the impact test barrel bore, which varied from 0.032 to 0.132 in., the impact angles did vary as indicated in the table. As indicated, capsules A-1a, A-4a, and A-5a included the impact absorber, the rest did not. Pt-10Rh was included on some capsules as indicated.

The sketch in Figure 6 illustrates the method used for determining the axial and diametral strain. Measurement of the capsule, prior to and post-test, were determined with vernier calipers and standard micrometers.

The impact energy is derived from $E = 1/2\ MV^2$; where

$$M = \frac{\text{Capsule Weight}}{32.2\ \text{ft/sec}^2}$$

V = Capsule Velocity, ft/sec

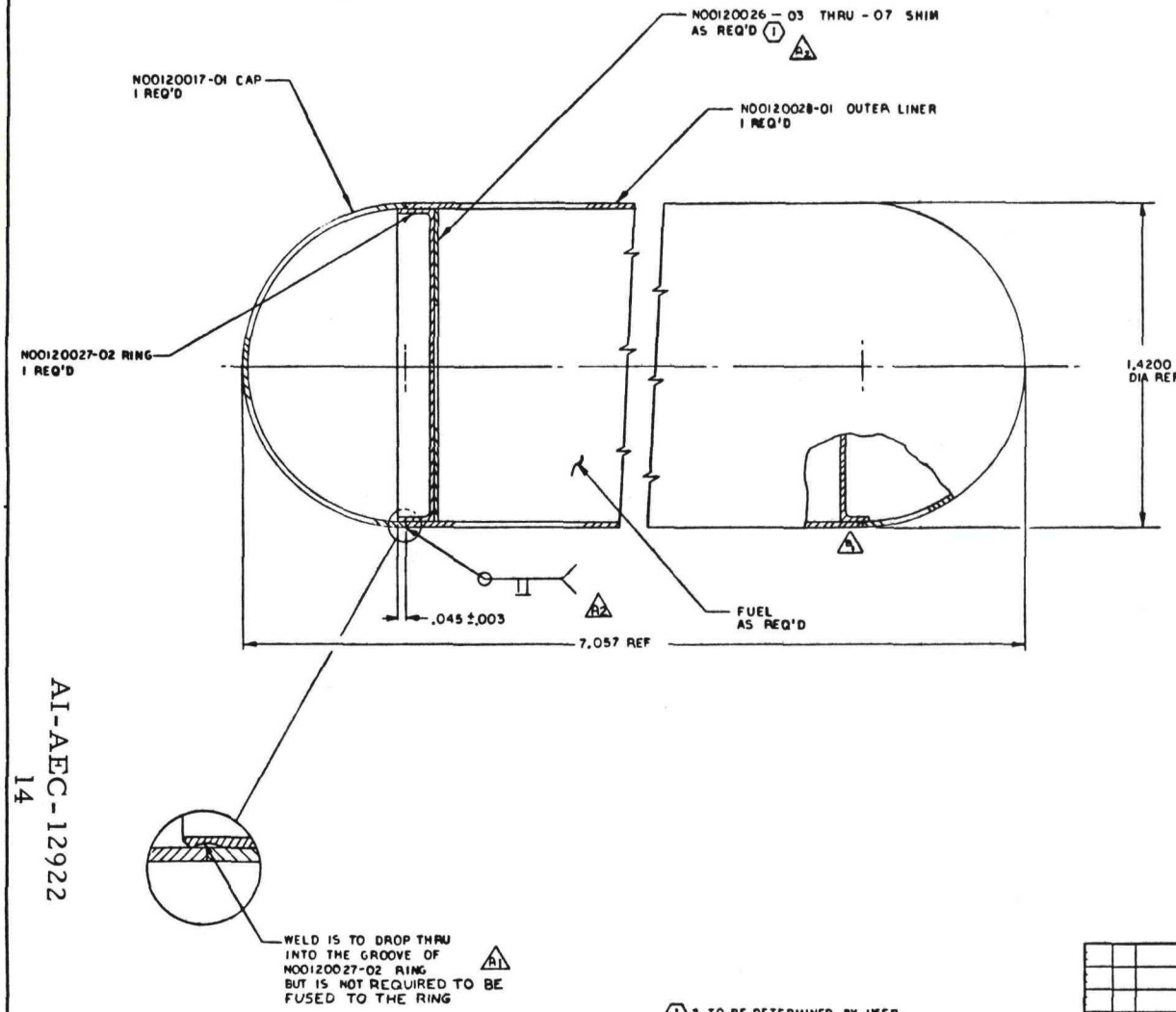

REVISIONS			
SYM	DESCRIPTION	DATE	APPROVED
B	SEE REVISION RECORD EO-55914	1-7-69 G BURNETT 3-6-69	

FOR INFORMATION
WILL NOT BE REPLACED AND MAY
BE CHANGED WITHOUT NOTICE

QTY REQD	PART OR IDENTIFYING NO.	NOMENCLATURE OR DESCRIPTION	CODE IDENT	MATERIAL	DATA: SPECIFICATIONS SIZES, NOTES, VENDORS	LINE NO.
(1) AS REQ		FUEL				
(1) AS REQ	N00120026 – 07	SHIM				
	– 06					
	– 05					
	– 04					
(1) AS REQ	N00120026 – 03	SHIM				005
1	N00120027- 02	RING				004
1	N00120028- 01	OUTER LINER SUB ASSY				003
1	N00120017- 01	CAP				002
	N00120029-01	ASSY				001

LIST OF MATERIALS OR PARTS LIST

(1) 2. TO BE DETERMINED BY USER.

1. DWG INTERPRETATION PER STO11SNA0015.
NOTES: UNLESS OTHERWISE SPECIFIED

ITEM	QTY	MODEL	NEXT USING DRAWING
		REQD PER END ITEM	
-01	1	001	N00120013

APPLICATION (USAGE) DATA

UNLESS OTHERWISE SPECIFIED: DIMENSIONS ARE IN INCHES. TOLERANCES ON: DECIMALS ANGLES FRACTIONS
XX = ± .03 ±30' ±1/32
XXX = ± .010
HOLES NOTED "DRILL"
.013 THRU .040 : ± .001 – .001
.041 THRU .130 : ± .002 – .001
.131 THRU .229 : ± .003 – .001
.230 THRU .500 : ± .004 – .001
.501 THRU .750 : ± .005 – .001
.751 THRU 1.000 : ± .007 – .001
1.001 THRU 2.000 : ± .010 – .001
DO NOT SCALE PRINT

DR BY G BURNETT 5/8/69
CHK BY 5-20-69
APPROVED BY

ATOMICS INTERNATIONAL

CODE IDENT NO. 09974 | SIZE D | N00120029 | SCALE 4/1 | SHEET

N00120029 B

AI-AEC-12922
14

Figure 5. Outer Liner Assembly – Large Volume

TABLE 1

IMPACT TEST SERIES SUMMARY

S/N	Impact Velocity (ft/sec)	Angle	Impact Temperature (°F)	Initial Length (in.)	Initial Diameter (in.)	Wall (in.)	Final Length (in.)	Final Diameter (in.)	Diameter Strain (%)	Axial Strain (%)	Mass (lb)	Impact Energy (ft/lb)	With Pt-10Rh	Summary
A-1a	250	30°	1200	7.375	1.676	0.127	6.836	1.926	14.8	21.2	4.8	4,680	Yes (Cap)	T-111 and Pt-Rh Leak Tight (included impact absorber)
A-2a	250	10°	1200	7.376	1.677	0.127	6.750	1.928	15.0	28.7	4.7	4,720	Yes (Cap)	T-111 Leak Tight
A-3a	260	End On	1200	7.372	1.676	0.127	6.610	1.972	17.4	26.4	4.7	4,940	Yes (Cap)	Leak Tight
A-4a	230	10°	1200	7.348	1.676	0.127	6.616	2.030	21.5	26.8	4.8	3,950	Yes (Cap)	Leak Tight (included impact absorber)
A-5a	240	End On	1200	7.325	1.624	0.100	6.624	1.919	18.2	29.0	4.0	3,600	No	Leak Tight (included impact absorber)
A-6a	260	43°	1200	7.323	1.625	0.100	6.525	1.932	18.9	33.8	4.0	4,200	No	Leak Tight
A-7a	346	End On	1200	7.419	1.718	0.127	6.100	2.115	26.5	42.2	5.2	9,700	Yes (Comp)	Leak Tight
A-8a	355	20°	1200	6.900	1.600	0.090	5.750	2.000	25.0	40.0	3.6	7,000	No	Leak Tight
A-9	357	43°	1200	7.049	1.540	0.060	6.000	2.052	24.9	53.2	3.23	7,650	No	Leak Tight
A-10	450	End On	1200	7.348	1.582	0.082	6.500	2.1305	25.75	22.78	3.50	11,000	No	Circumferential Crack on Impact End
A-11	400	End On	1200	7.342	1.582	0.082	6.750	2.075	23.76	19.59	3.51	8,700	No	Circumferential Crack on Impact End
A-24	353	24°	1200	7.060	1.584	0.082	6.000	1.986	20.3	60.3	4.44	8,600	No	Fully Packed with Fuel Leak Tight

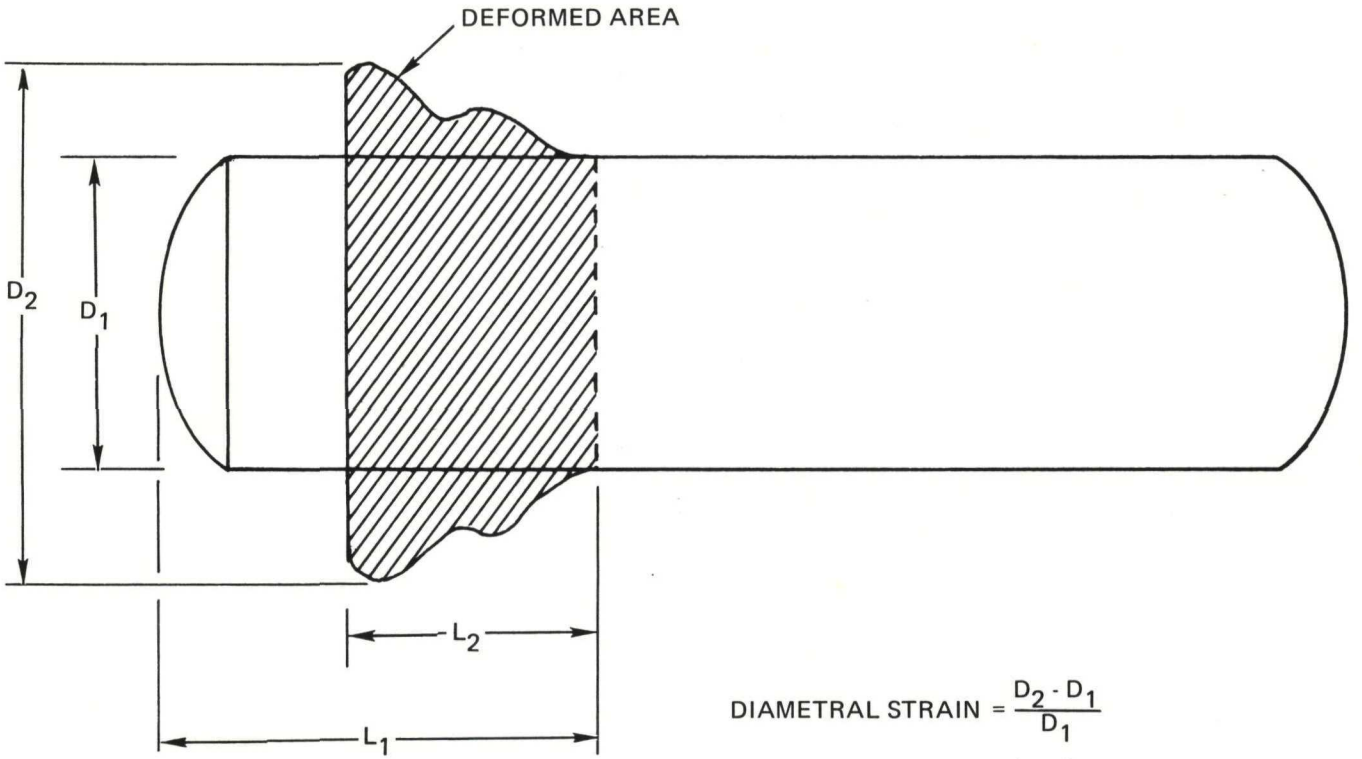

$$\text{DIAMETRAL STRAIN} = \frac{D_2 - D_1}{D_1}$$

$$\text{AXIAL STRAIN} = \frac{L_1 - L_2}{L_1}$$

WHERE: D_1 = ORIGINAL DIAMETER OF STRUCTURE

D_2 = DIAMETER OF DEFORMED AREA

L_1 = ORIGINAL LENGTH OF AREA THAT WAS DEFORMED

L_2 = LENGTH OF THE DEFORMED AREA

Figure 6. Model for Determining Axial and Diametral Strain

IV. POST-TEST EXAMINATION

A. VISUAL EXAMINATION AND HELIUM LEAK TEST

Each impact capsule was visually examined immediately following the impact test and again after the capsule was cool enough for close examination. In the first ten tests the visual examination indicated the capsule's structural shell to be unbreeched. A-10 and A-11, the final two high velocity capsules were breeched, apparently by a shear failure mode.

Following the visual examination, each impact capsule was helium leak tested. The leak test consisted of externally pressurizing the capsules to 100 psig helium and maintaining the pressure for 30 minutes. This was followed by submerging the capsules in alcohol to remove residual helium. The capsules were helium leak tested in a vacuum chamber connected to a leak detector. All the capsules except A-10 and A-11 were leak tight.

B. DISASSEMBLY AND INTERNAL EXAMINATION

The first six capsules were impacted at relatively low velocities (230 to 260 ft/sec). A typical pre-test configuration for these "A" capsules (Al_2O_3 coated but no Pt-10Rh clad) is shown in Figure 7. The impacted capsules are shown in Figures 8 through 13. Four of these were 0.127 and two were 0.100-in. wall capsules. Two of the 0.127 capsules (A-1a and A-4a) and one of the 0.100 capsules (A-5a) contained foamed Ta-10W impact absorbers at the impact end. The capsules were sectioned after testing to determine the effect of the impact absorber on the amount of deformation incurred and also to determine the integrity of the inner and outer liner assembly. The amount of deformation incurred by the T-111 structures appeared unaffected by the presence of the impact absorber. It appears, however, that the liners incur more deformation when the absorber is used. The impact absorber was omitted on all of the other impact capsules.

In fabricating the first six capsules, with the exception of A-3a, the fuel retainer ring to the outer liner and was not welded with sufficient penetration to withstand impact. However, all of the cap to liner welds and the retainer ring to inner liner welds were intact after impact. The parameters for the

outer liner to fuel retainer weld were adjusted to provide deeper penetration on the remaining impact capsules.

Of the Platinum-10% Rhodium oxidation barrier caps installed on the first four capsules, only A-1a survived impact in a leak tight condition. However, A-1a was the only barrier cap which was fully annealed, the others being impacted as drawn.

The second six capsules were impact at velocities ranging from 350 to 450 ft/sec. Impact capsule A-7a, Figure 14, was the first of the higher velocity impact capsules. The velocity was 345 ft/sec and the angle was end on. This was also the only capsule to include a complete Pt-10Rh oxidation barrier. The Pt-10Rh clad failed in tension at the end opposite impact (Figures 15 and 16) due to inadequate tensile strength. The higher tensile strength of Pt-20Rh may avoid this type of failure. The T-111 structural shell on A-7a was leak tight. The sectioned shell is shown in Figure 17.

Impact capsule A-8a, Figure 18, was the first 0.090-in. wall capsule and was impacted at 355 ft/sec at an angle of 20°. The capsule was leak tested following impact and was leak tight.

Impact capsule A-9 was a 0.060-in. wall capsule. It was impacted at 357 ft/sec and at an angle of 43°. Figures 19 and 20 show this capsule after impact. It is evident from the photos that the capsule incurred a severe secondary impact. The leak test, however, showed that the capsule was leak tight. Half-sections of this capsule are shown in Figure 21.

Impact capsule A-24, Figure 22, was fully packed with fuel simulant when impacted. The fuel retainer rings were converted to discs and the inner liner was omitted. The capsule was impacted at 353 ft/sec and at an angle of 24°. The leak test of the capsule showed it to be leak tight after the impact test. Half-sections of the capsule are shown in Figure 23.

The impact velocities for capsules A-10 and A-11 were increased to determine a failure velocity and mode for the LRHSC design capsule. The impact velocity of A-10 was 450 ft/sec and the angle was end on. The failure took place in the dome of the impact end, Figure 24, and encompasses approximately 280° of the impact surface. The breech is due to a shear of one of the convolutions

formed at the impact end. Capsule A-11, Figure 25, was impacted at 400 ft/sec and was also end on. The breech was smaller but similar to that in A-10; i.e., the shear failure encompasses approximately 110° of the impact end. On both these capsules the tungsten-moly fuel simulant was completely contained.

C. METALLOGRAPHIC EXAMINATION

The first impact capsule to be examined metallographically was A-3a. The intent of this first examination was to determine the condition of the T-111 microstructure in the impact end. Figure 26 shows a full cross-sectional view of the impact end. The duplex structure seen here is not a result of the impact test but of the fabrication process. A duplex structure is typically found in the closed ends of deep drawn T-111 structural shells.[2] There was no evidence of cracks or microcracks in the T-111 structure, nor was there evidence of reduction in wall thickness at the new transition point of the impact surface and the side wall. The thickness of the wall of the T-111 structural shell below this point had a maximum increase of approximately 26%. The liner welds in A-3a all survived intact. Typical welds are shown in Figure 27. Some crack initiation in the liner parent material can be seen in Figure 27. This also was typical.

A-7a was examined metallographically to determine the amount of reduction in wall thickness at the transition of the impact end and the capsule side wall. Figure 28 shows the cross sectioned capsule. Figure 29 is a photomicrograph of the other half of the upper right hand corner showing the reduction in wall thickness in the corner. The amount of reduction is approximately 40%. This is the type and location of wall thinning which led to the shear failures in the higher velocity A-10 and A-11 capsules.

It can readily be seen in Figure 28 that the Ta-10W liner was deformed considerably without the welds failing. The outer liner, however, is very close to being sheared in one place. There was one shear failure in either the inner or the outer liner of each capsule impacted in the 350 ft/sec range.

Figure 30 shows the impact end of A-8a and the shear of the inner liner. Figure 31 is a photomontage of micrographs for the other half of the upper right hand corner of Figure 28. The T-111 material has exhibited a high degree of both ductility and strength to have permitted the amount of deformation exhibited

in Figure 31 without failure or even crack propagation. The inner liner failure shown in this figure can also be seen in the photomacrograph of the previous figure and is a transgranular tensile failure.

Capsule A-9, the 0.060-in. wall capsule was shown in Figure 21. A magnification of the upper corner of the impact end is shown in Figure 32.

This capsule was the first to be impacted on an angle near 45°. The T-111 thinned approximately 35% at the sharpest bend. The Ta-10W liner welds and material were very ductile even though the inner liner to fuel retainer ring weld is near failure. This capsule again is a demonstration of the very large amounts of deformation the T-111 will sustain without failure.

The impact capsule with the fully packed cylindrical section, A-24, is shown metallographically in Figure 33. Note the multiple bellows foundation at the impact end. The amount of reduction in wall thickness at the edge of the impact surface is approximately 40%. Removal of the inner liner was not detrimental to the capsule's survivability with the tungsten-moly fuel simulant.

The Ta-10W liner welds are shown typically prior to impact in Figure 34 and post-impact in Figure 35. All of the welds were formed by an electron beam process and have exhibited a high resistance to failure when impacted.

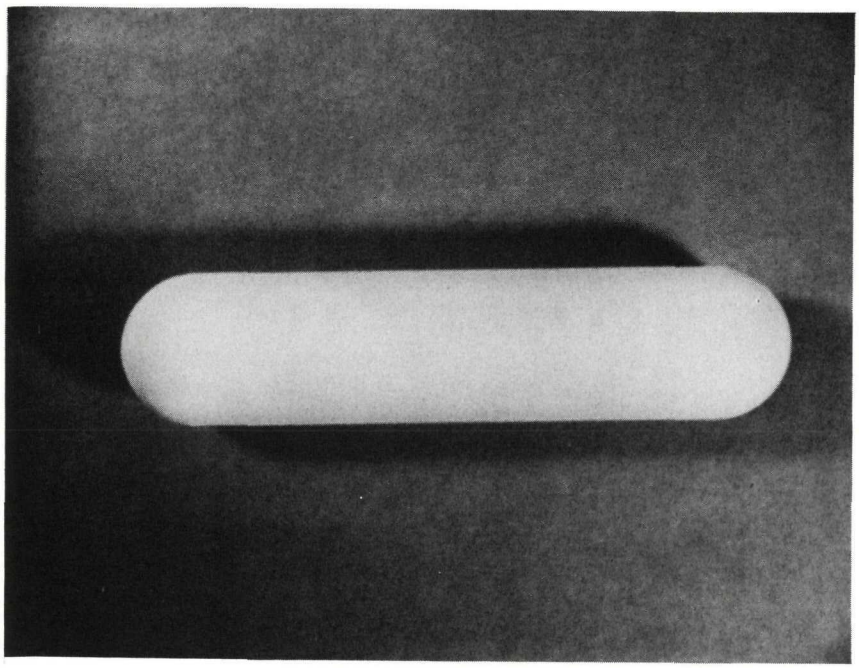

Figure 7. Impact Capsule with Al_2O_3 Coating Applied

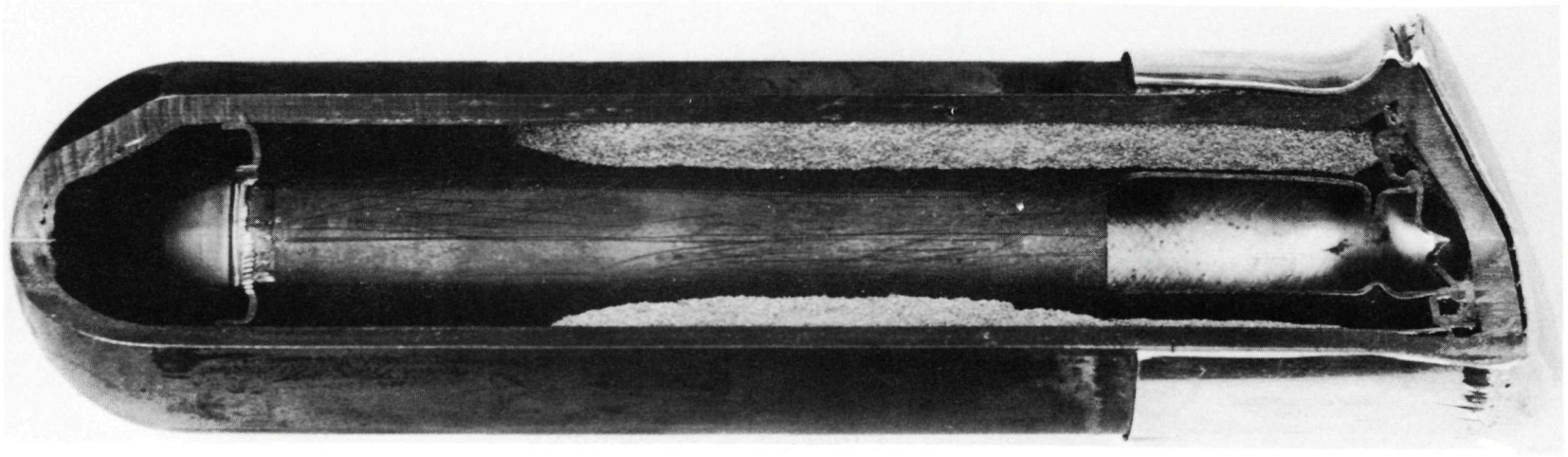

Figure 8. Impact Capsule A-1a

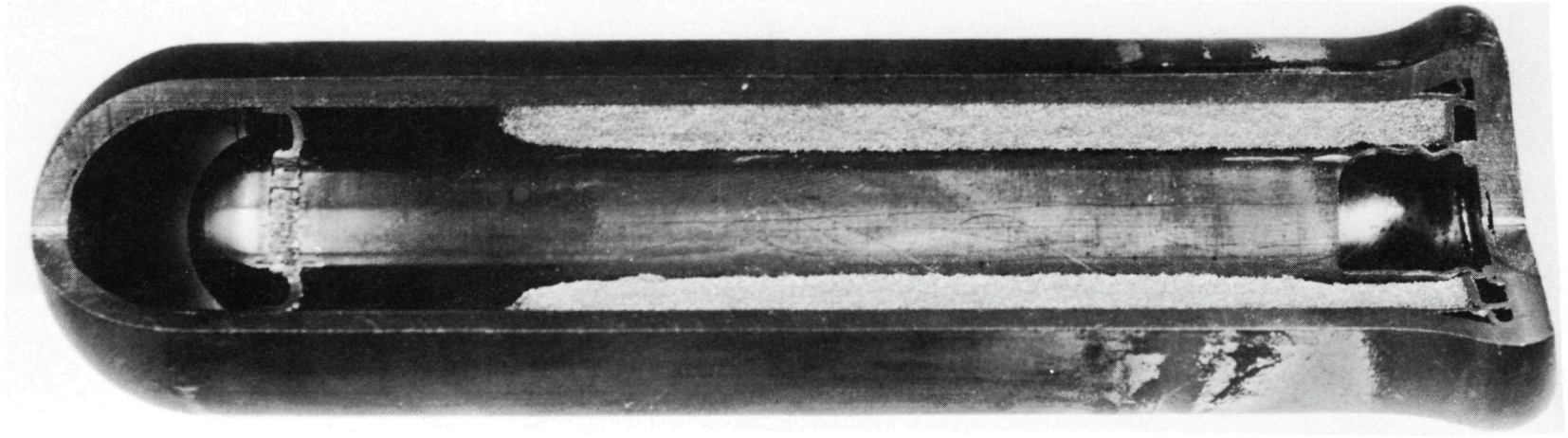

Figure 9. Impact Capsule A-2a

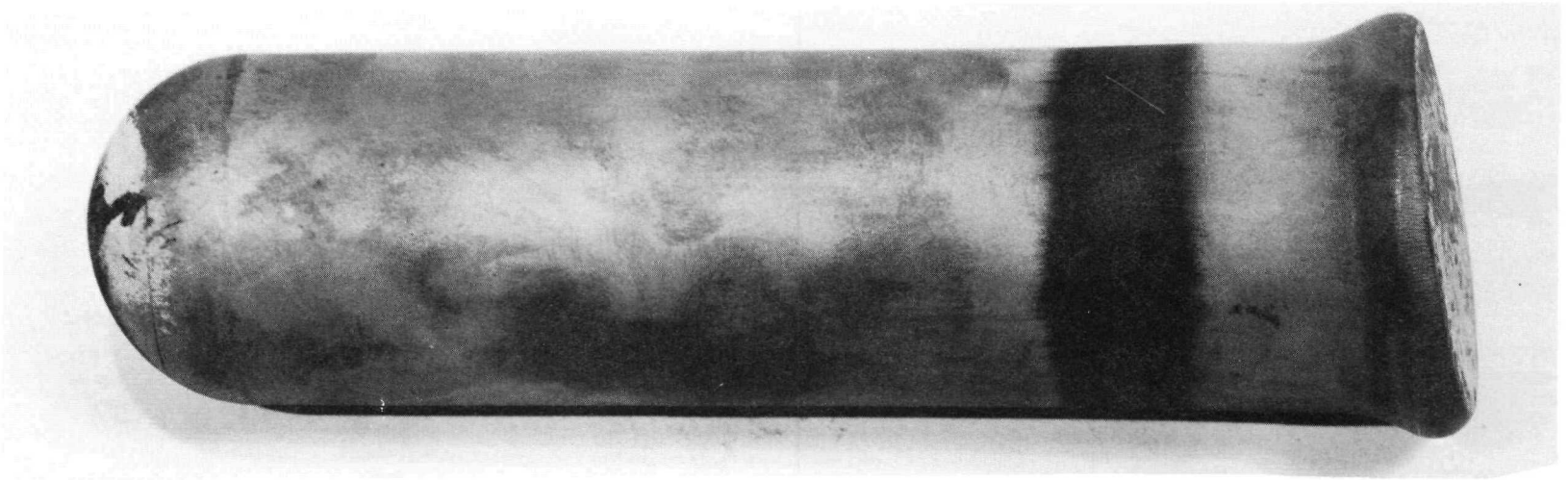

Figure 10. Impact Capsule A-3a

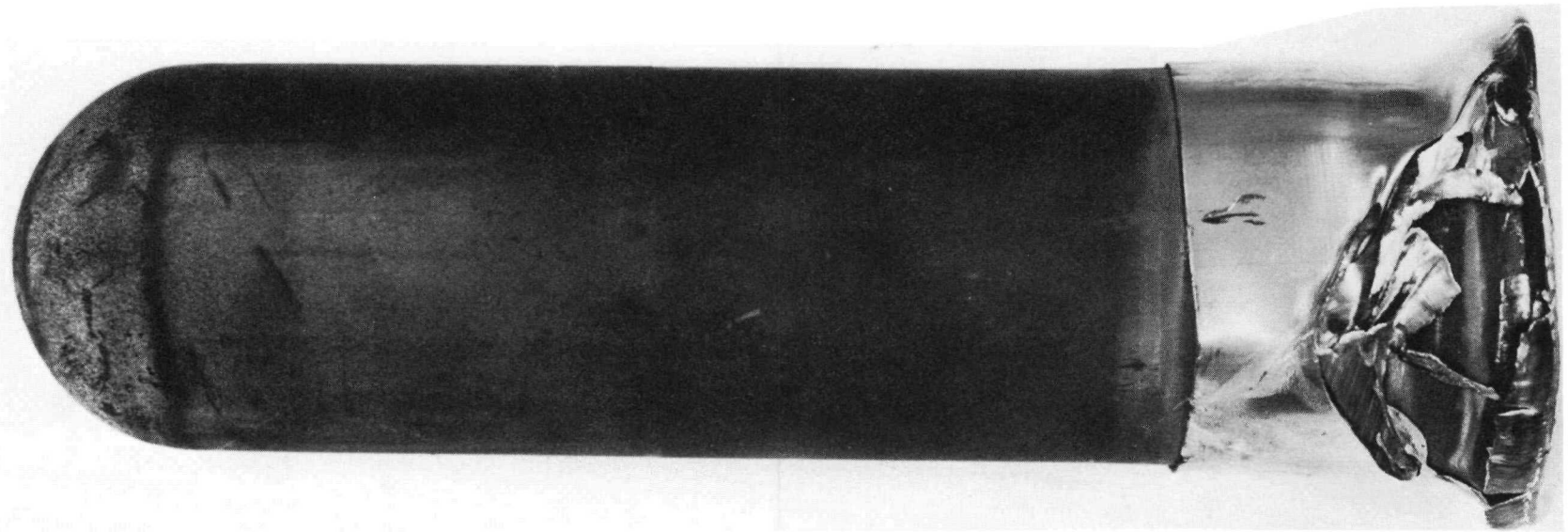

Figure 11. Impact Capsule A-4a

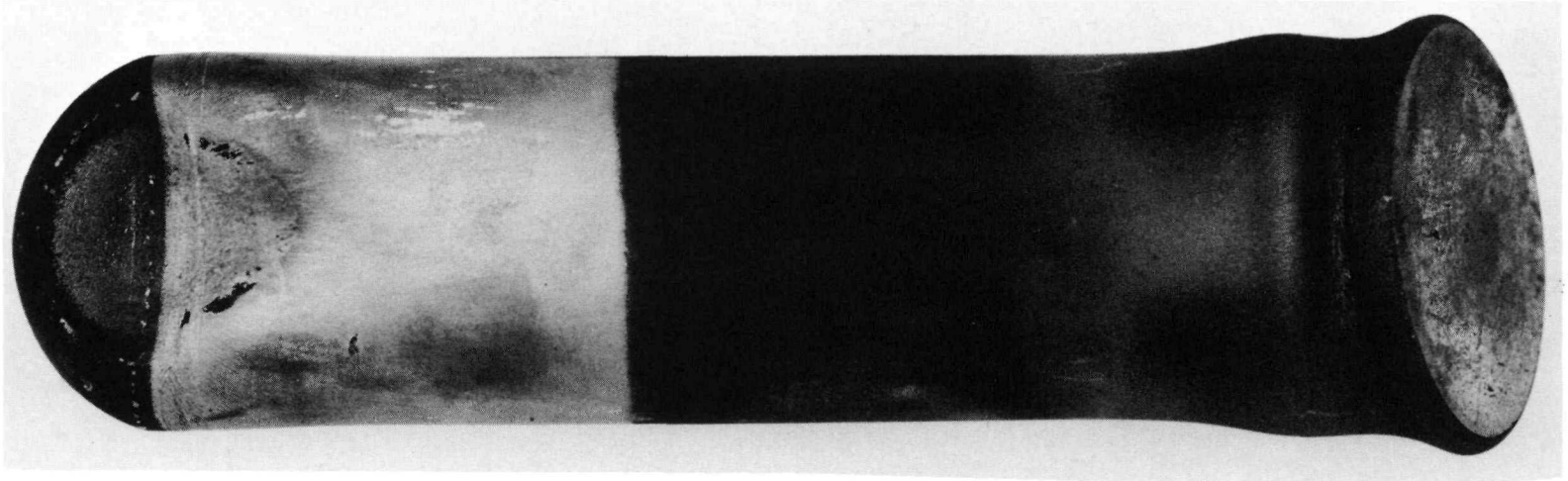

Figure 12. Impact Capsule A-5a

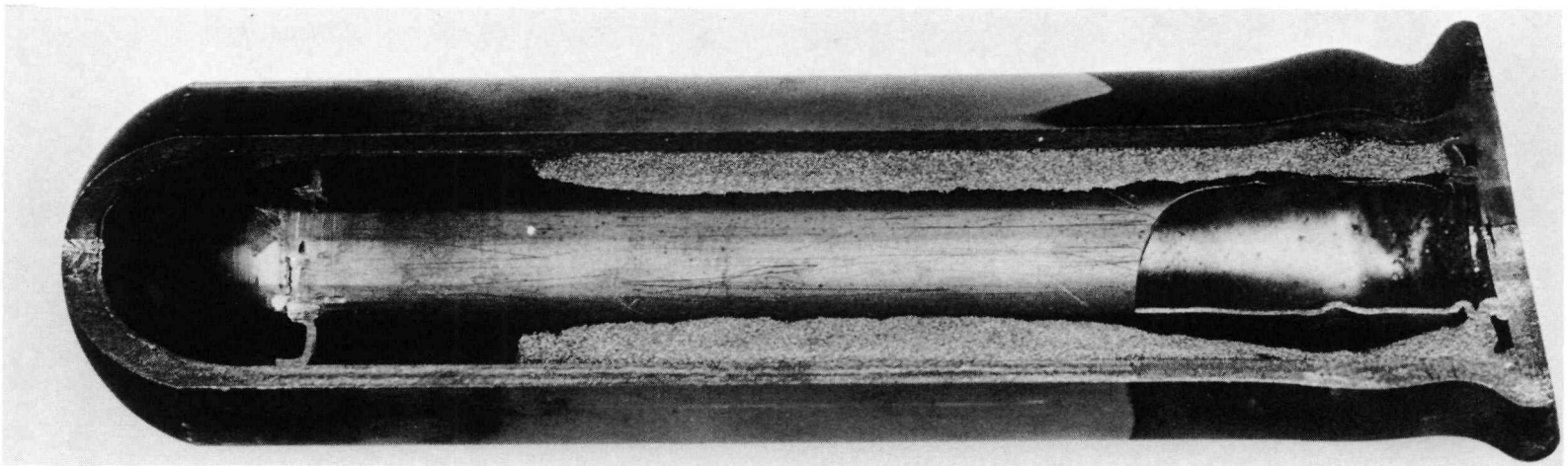

Figure 13. Impact Capsule A-6a

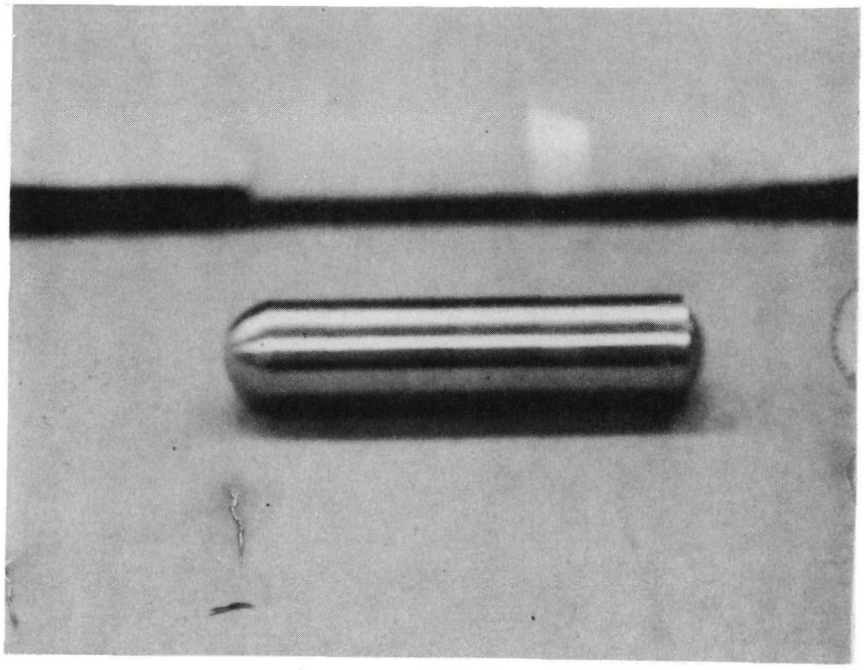

Figure 14. Impact Capsule A-7a Inserted in the Pt-Rh Barrier Shell and Cap

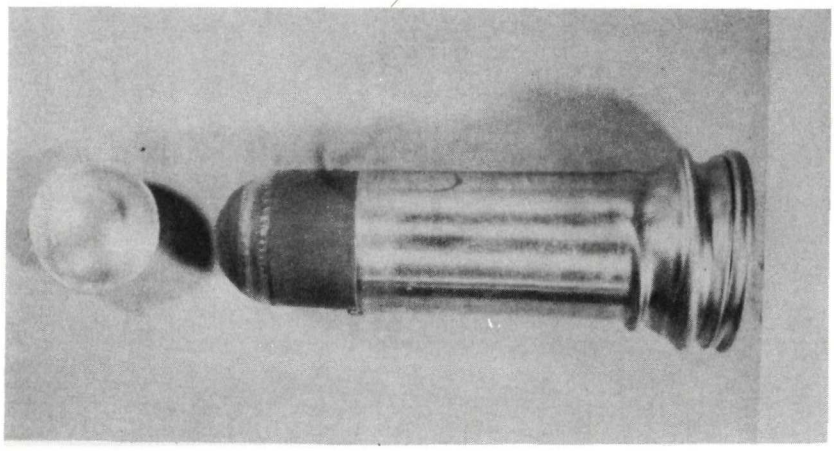

Figure 15. Impact Capsule A-7a After Impact Testing at 1200°F at 346 ft/sec

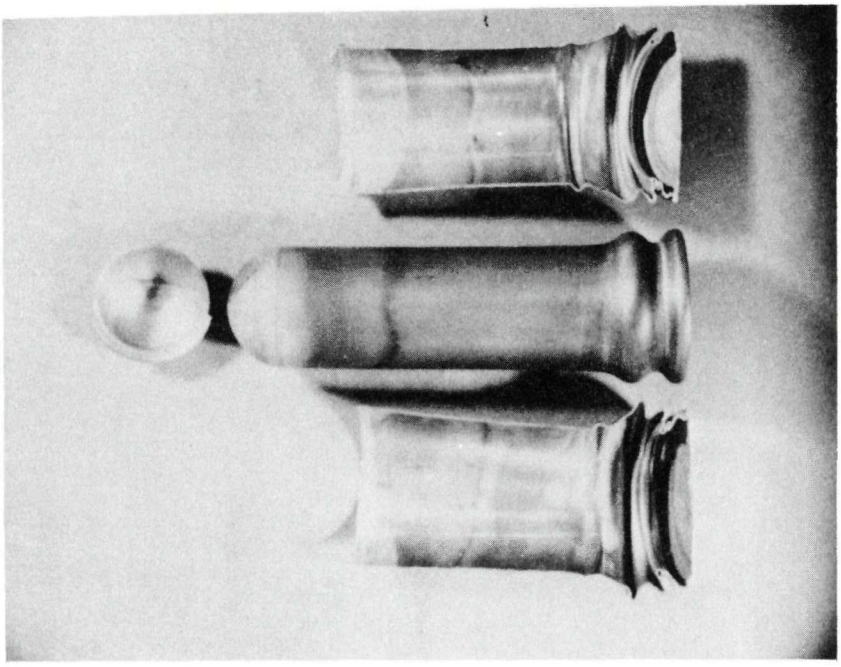

Figure 16. Impact Capsule A-7a with the Pt-Rh Removed

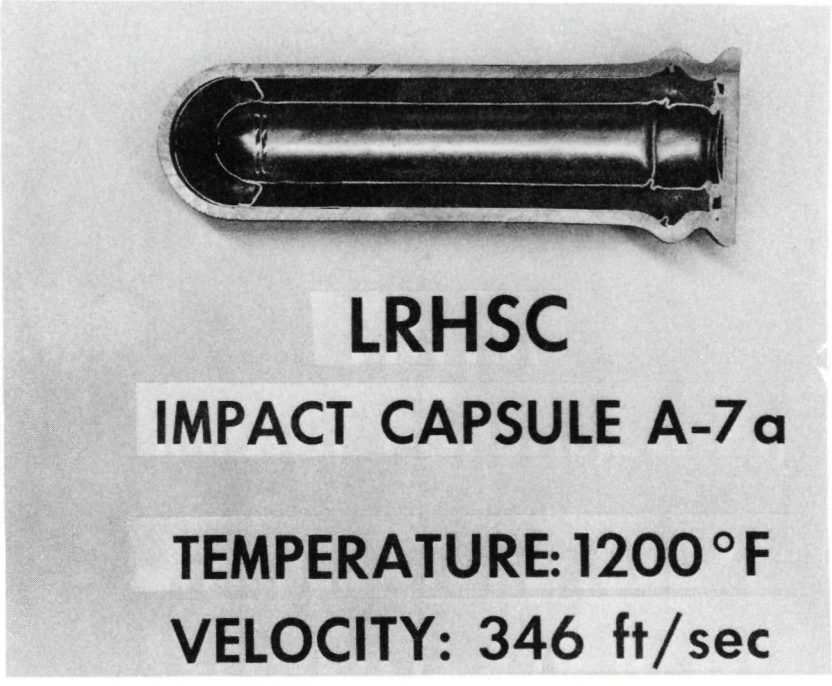

4-9-69 7734-4059

Figure 17. Impact Capsule A-7a

7734-4067

Figure 18. Impact Capsule A-8a

Figure 19. Impact Capsule A-9 After Test

Figure 20. Impact Capsule A-9 After Test

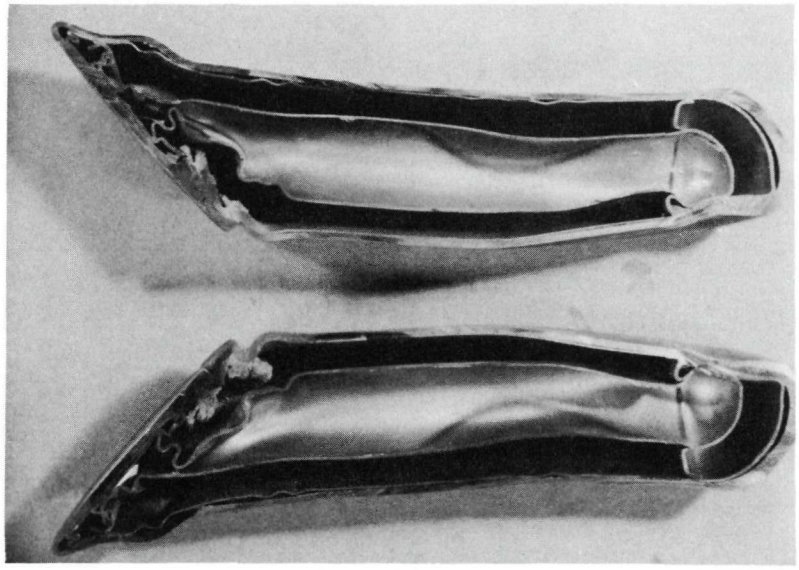

Figure 21. Half Section of Impact Capsule A-9

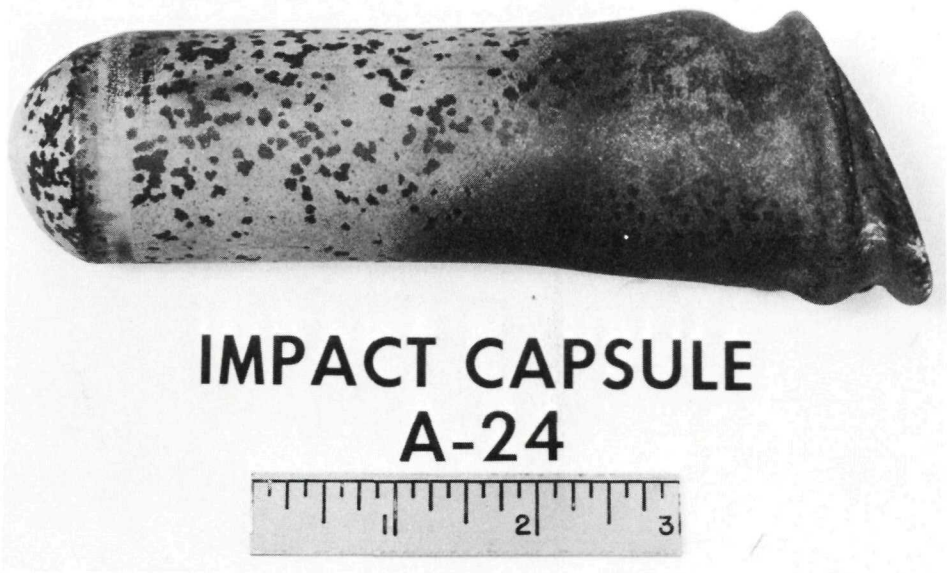

Figure 22. Impact Capsule A-24 After Test

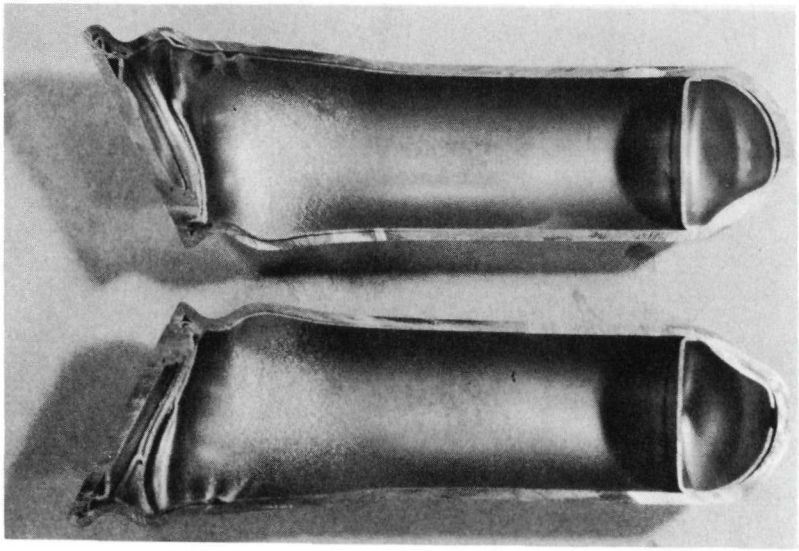

Figure 23. Half Section of Impact Capsule A-24

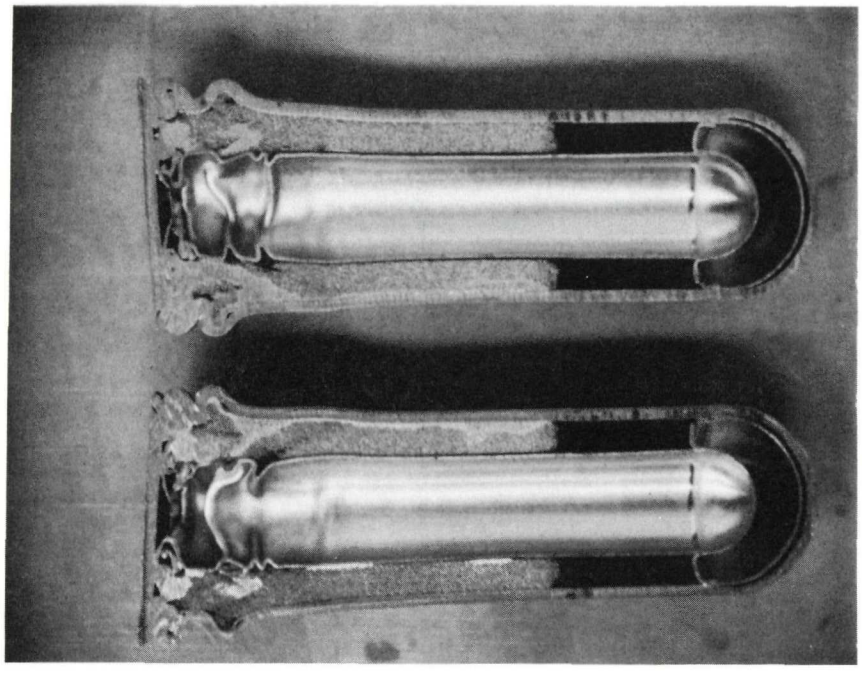

Figure 24. Impact Capsule A-10

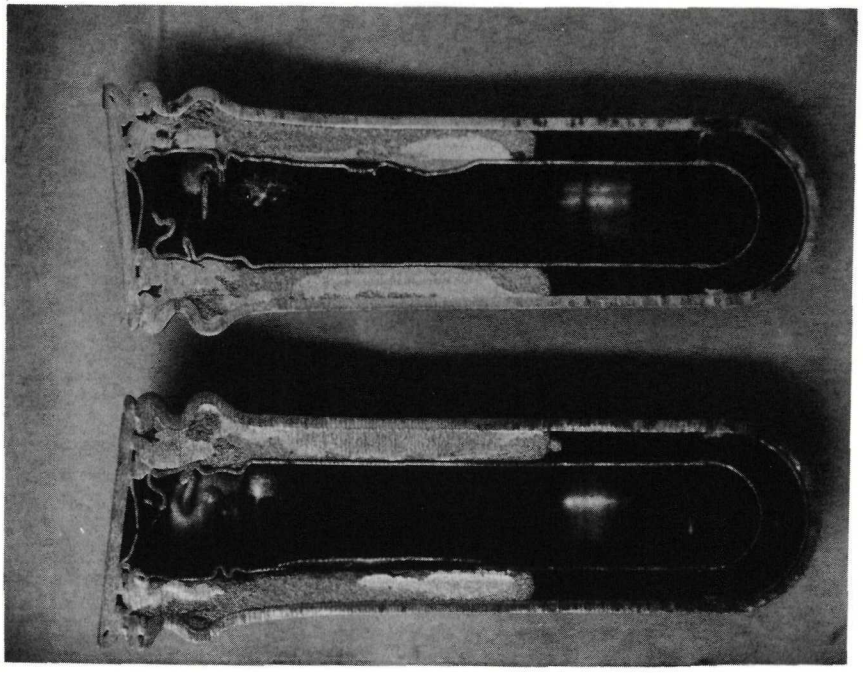

Figure 25. Impact Capsule A-11

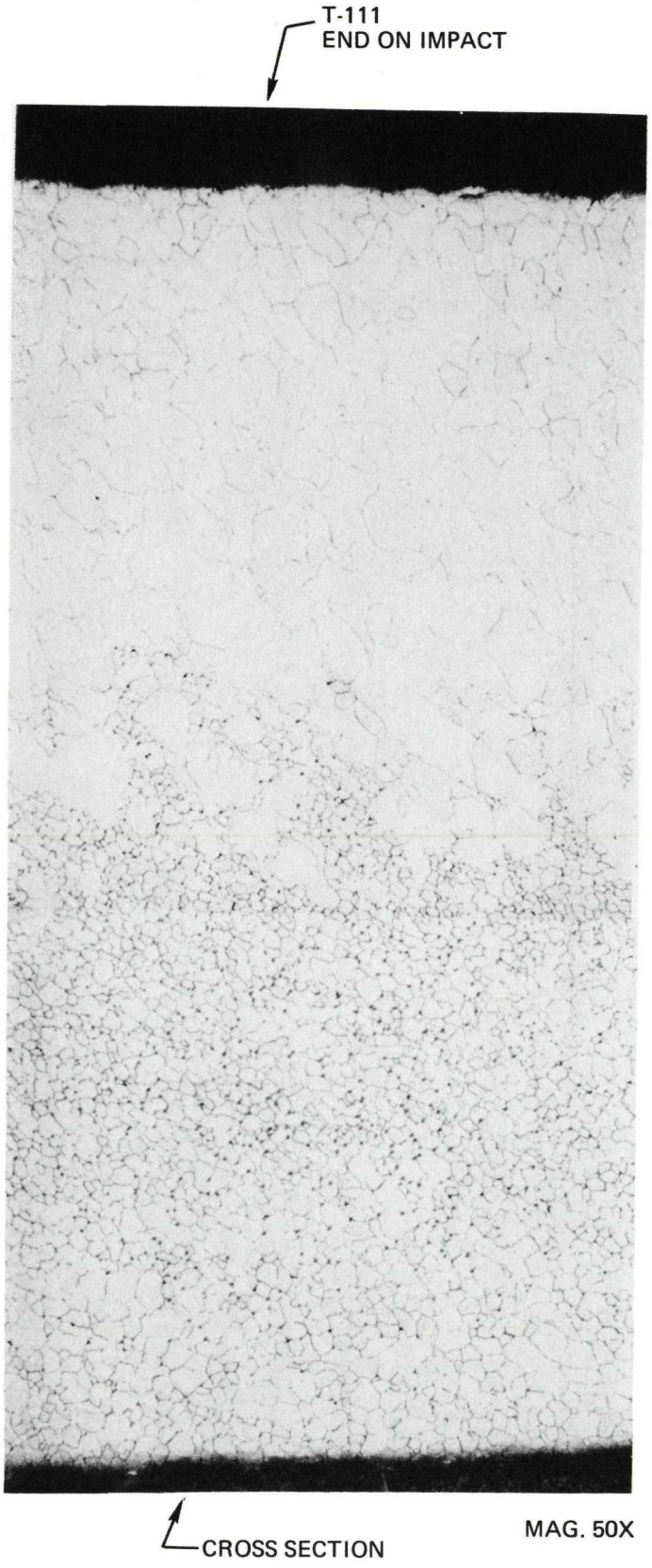

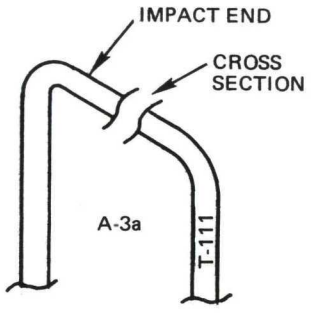

Figure 26. Microstructure of Impact End at A-3a

PAGE BLANK

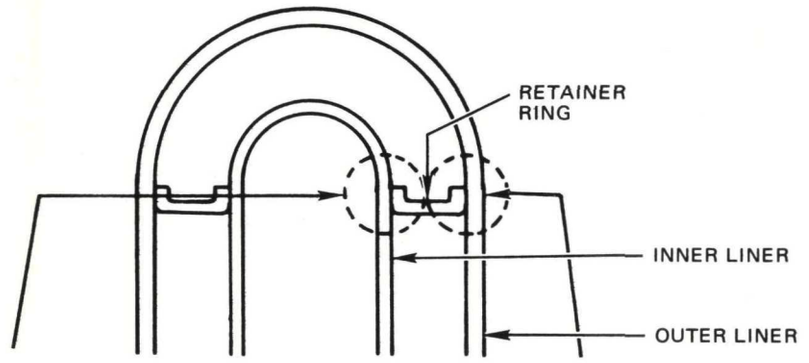

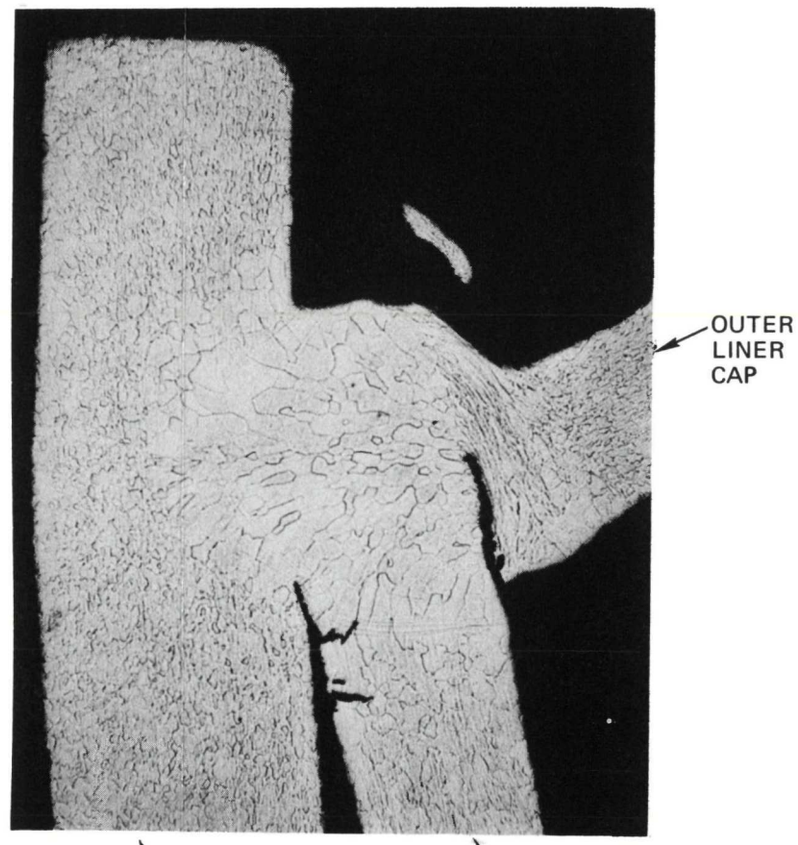

Figure 27. Ta-10W Inner and Outer Liner Welds of Impact Capsule A-3a

PAGE BLANK

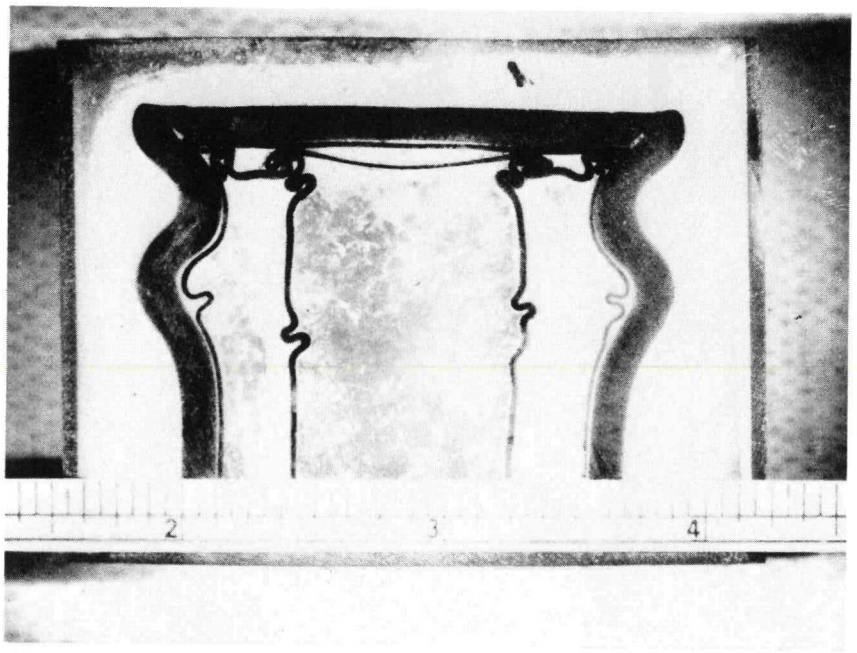

Figure 28. Impact End of A-7a

PAGE BLANK

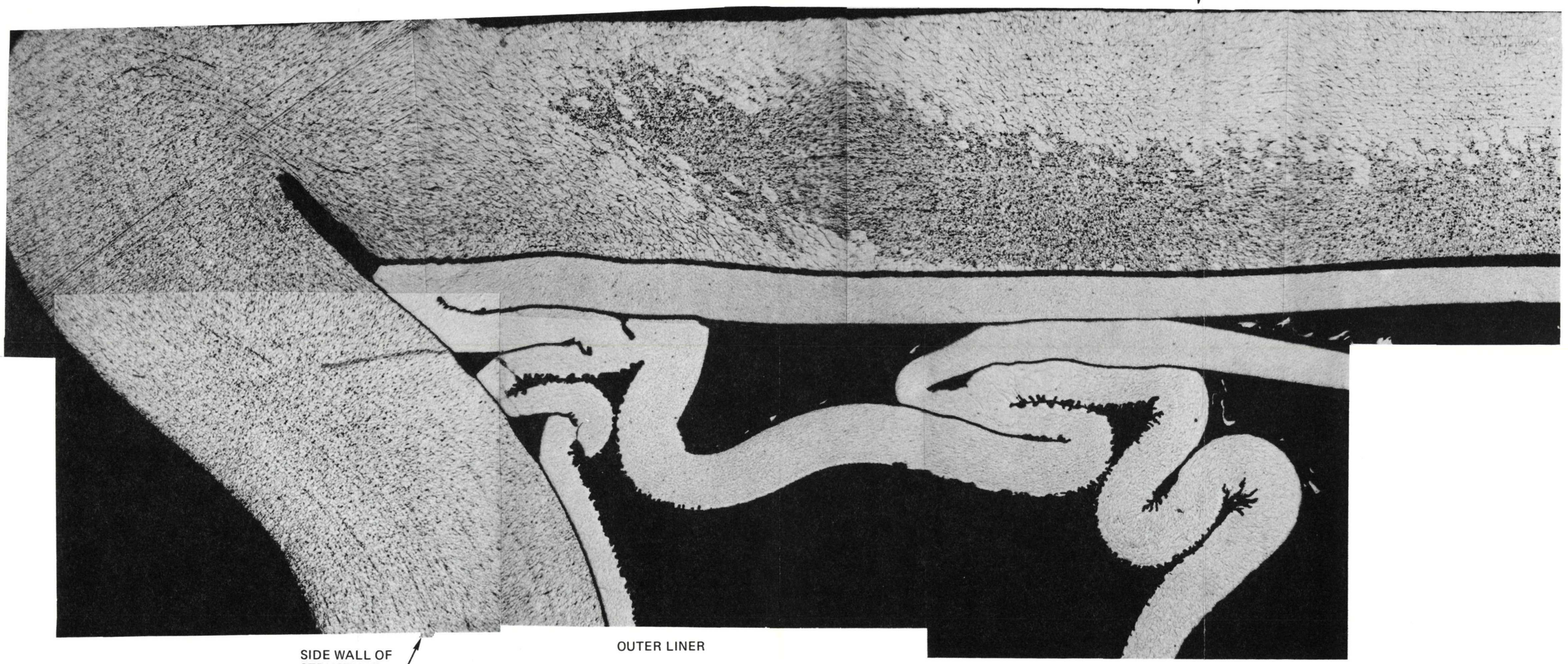

Figure 29. Photomacrograph of A-7a

PAGE BLANK

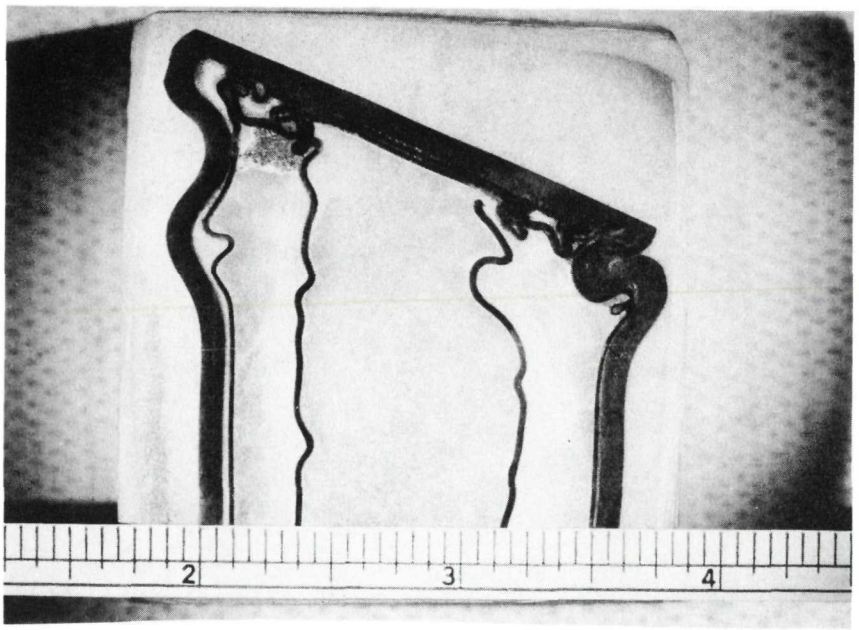

Figure 30. Photomacrograph of A-8a

PAGE BLANK

MAG. 16X

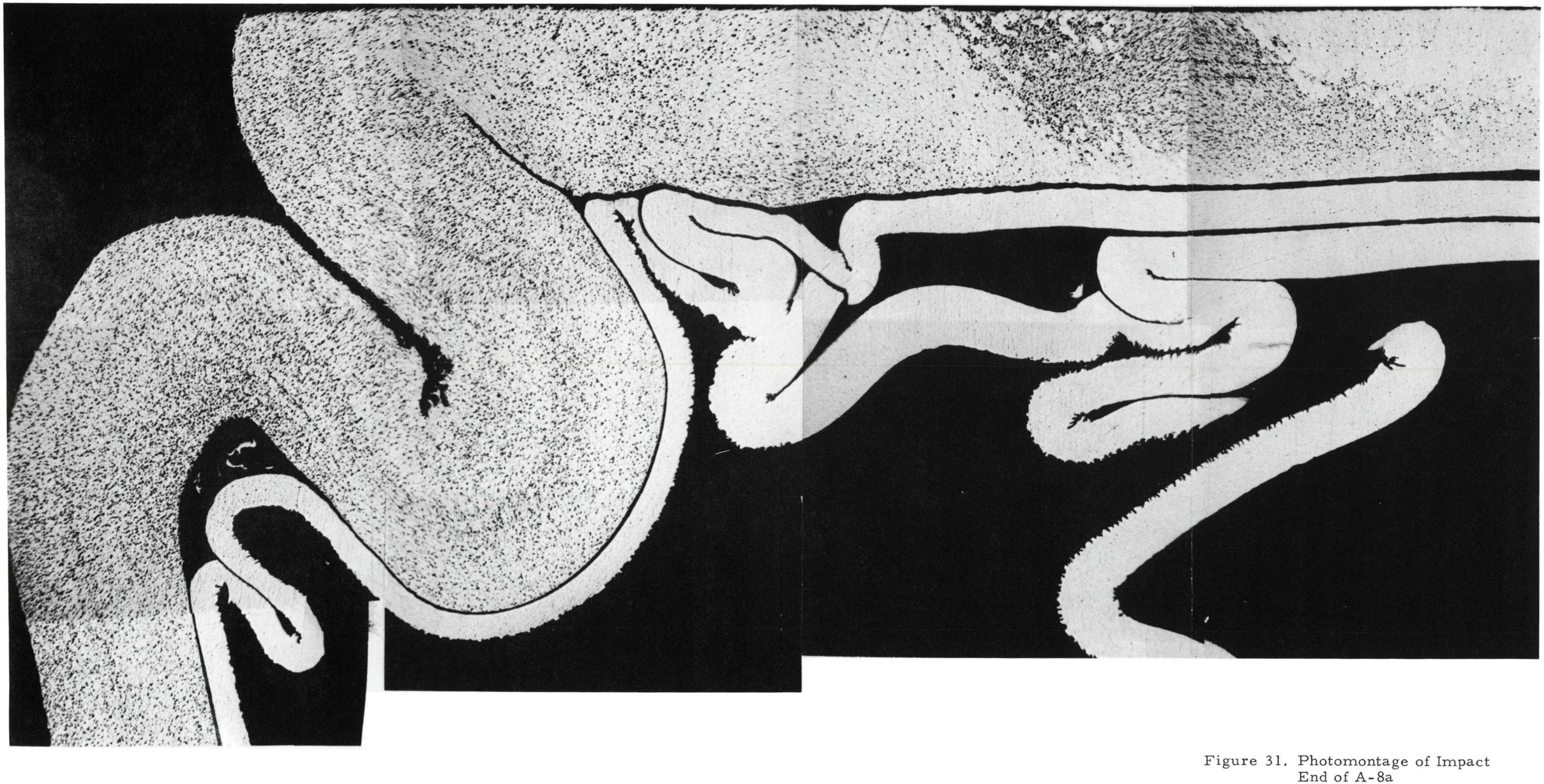

Figure 31. Photomontage of Impact End of A-8a

PAGE BLANK

MAG. 25X

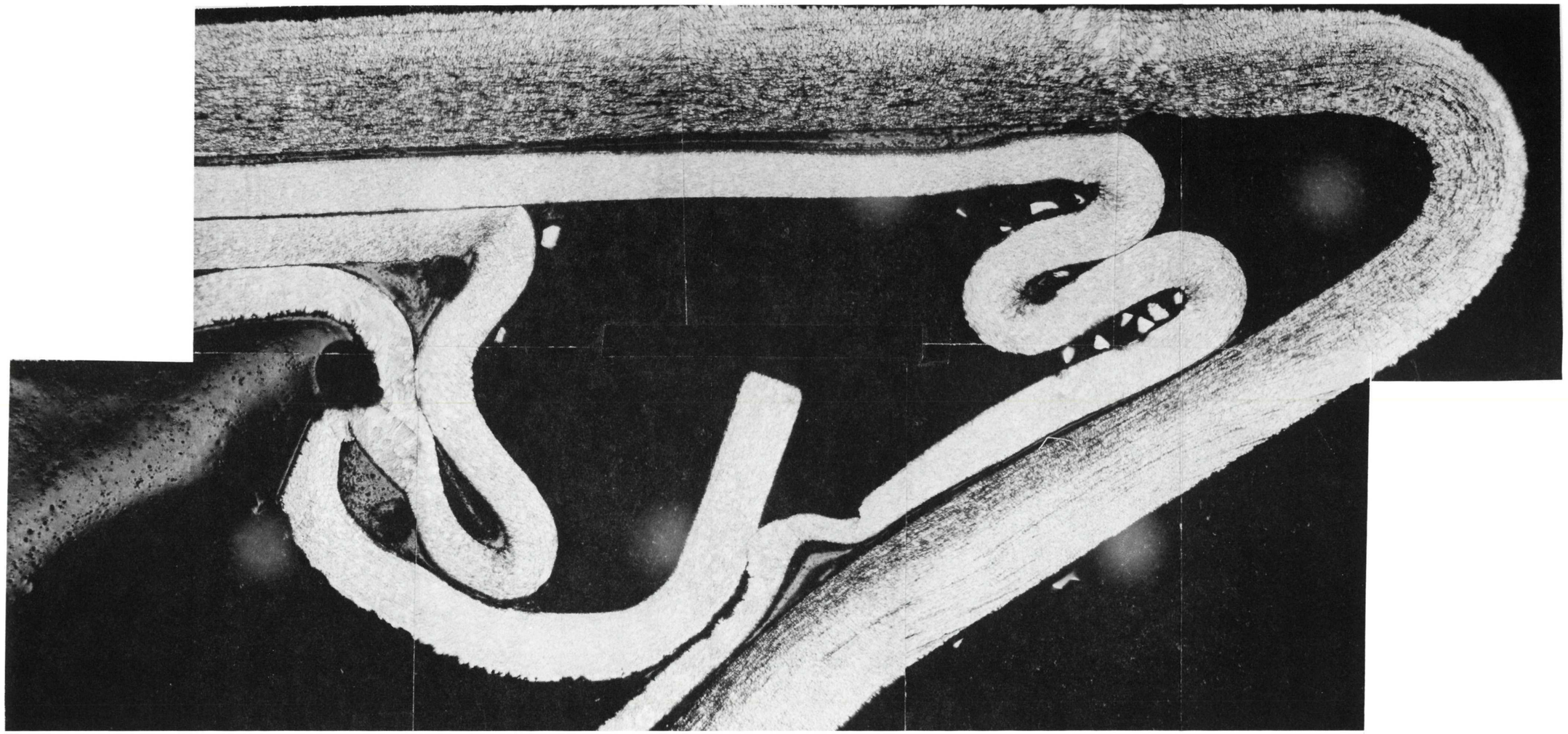

Figure 32. Photomontage of Impact End of A-9

PAGE BLANK

MAG. 16X

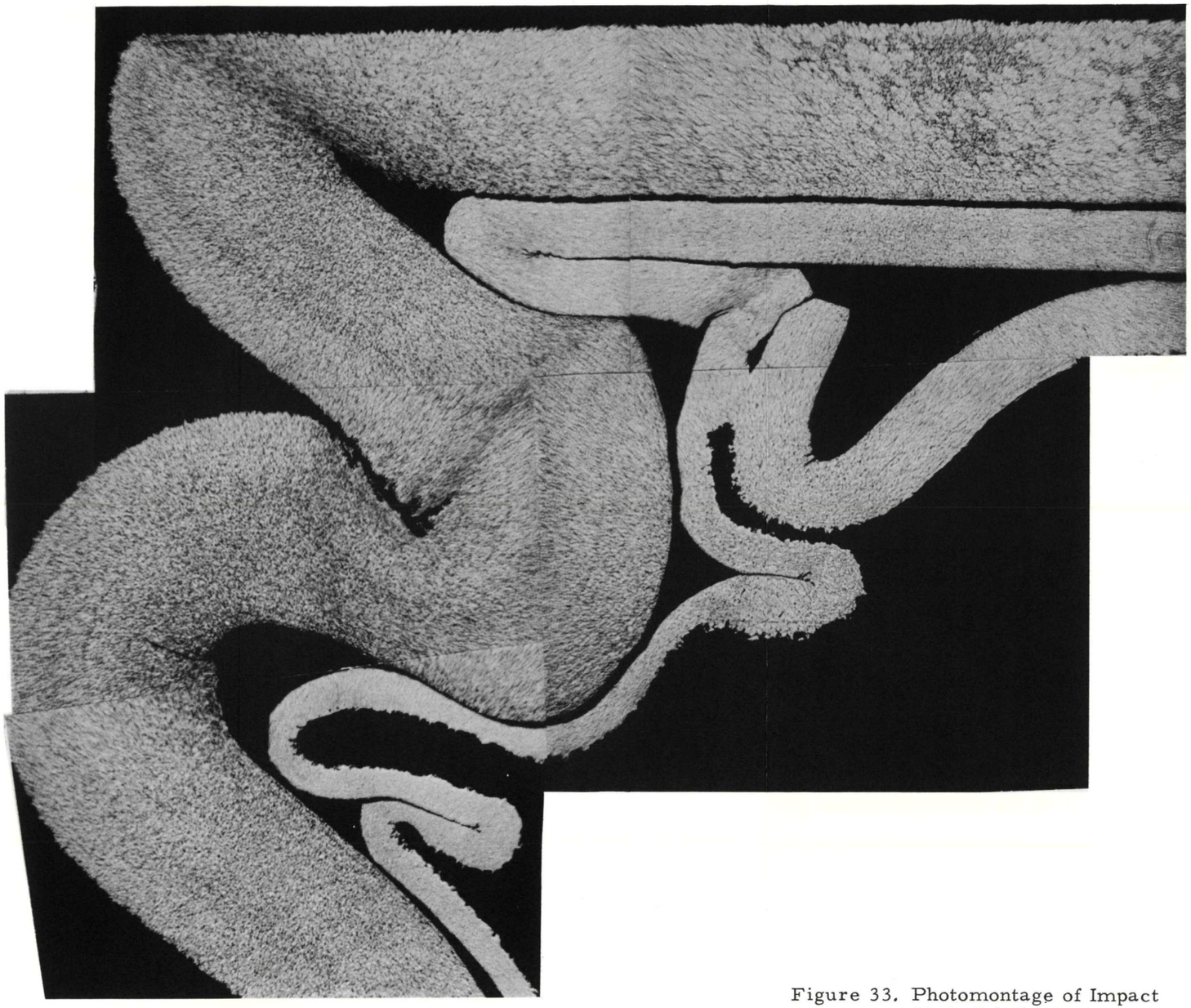

Figure 33. Photomontage of Impact End of A-24

PAGE BLANK

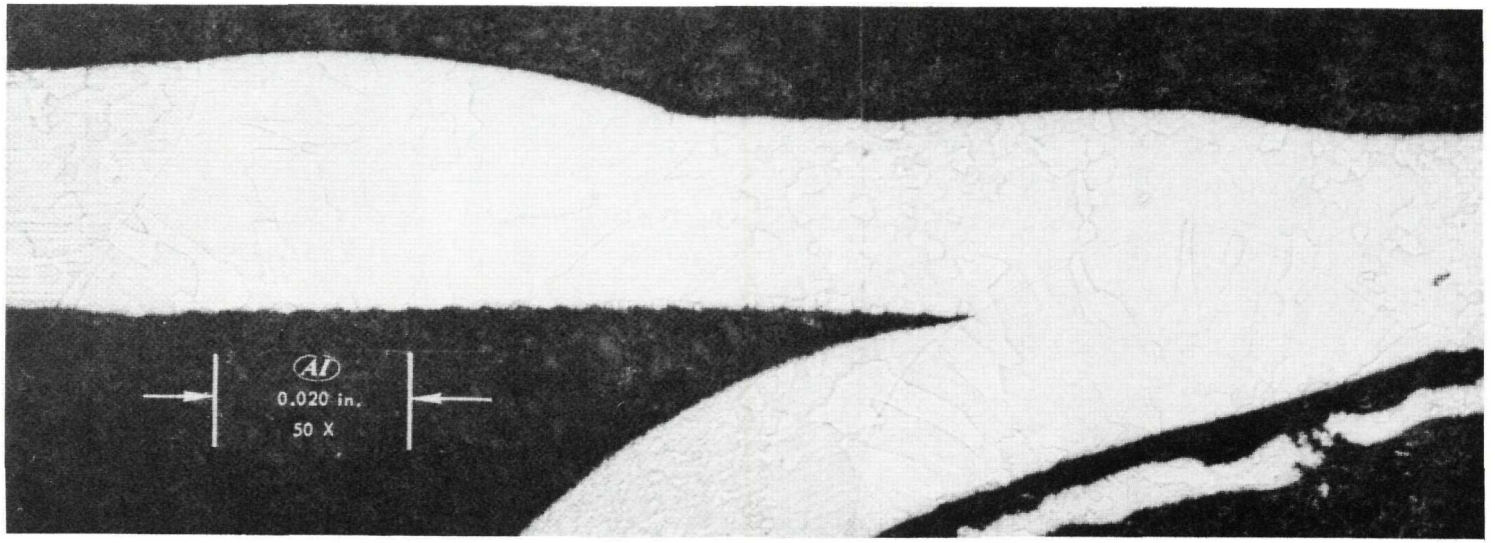

a. Inner Liner to End Cap Weld and
Inner Liner to Fuel Retainer Ring Weld

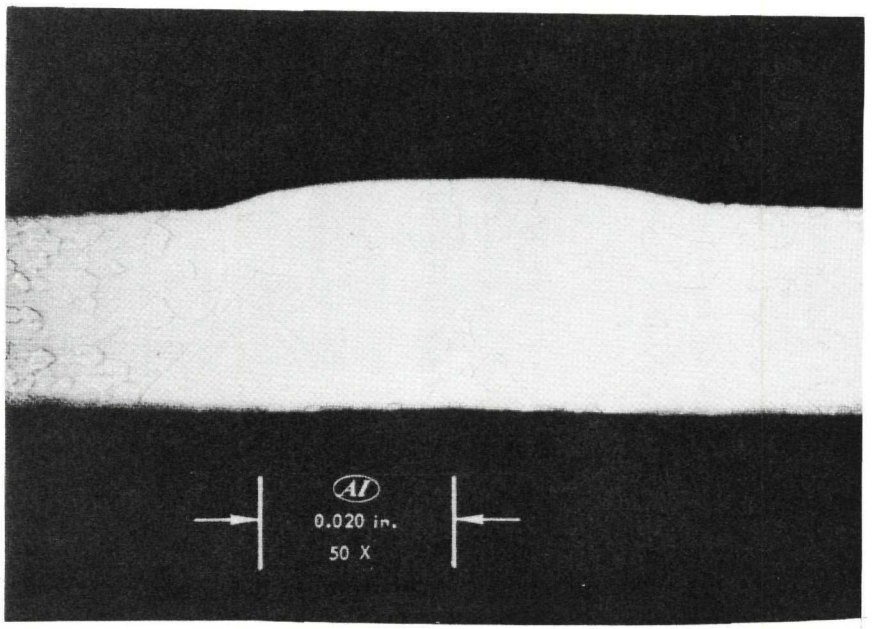

b. Outer Liner to End Cap Weld

Figure 34. Ta-10W Liner-End Cap-Retainer Ring Welds

PAGE BLANK

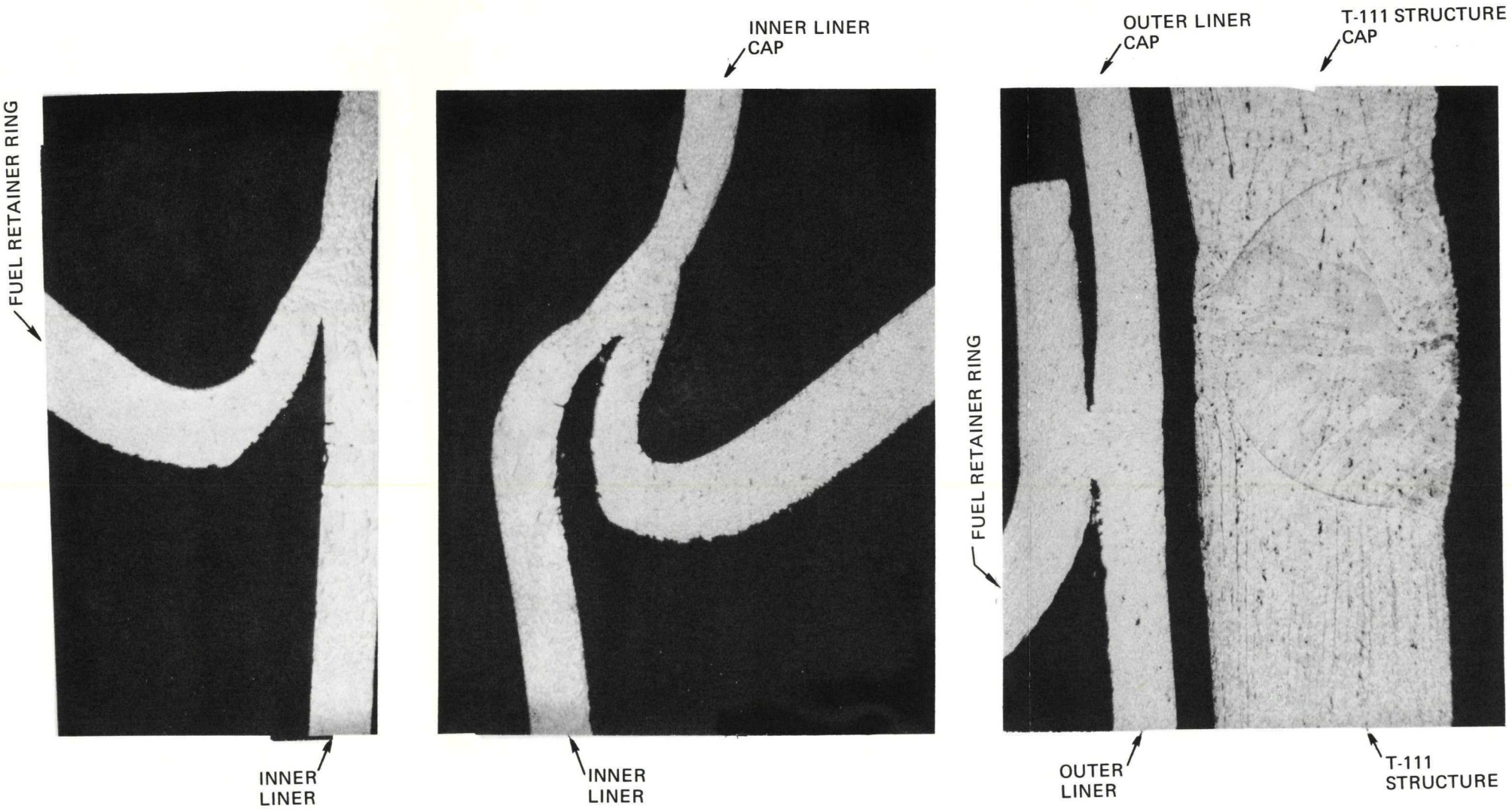

Figure 35. Typical Post-Impact Liner Welds

PAGE BLANK

V. IMPACT ENERGY DISTRIBUTION

Comparison of the maximum energy absorbing capability of the structural material in a fuel capsule with the total kinetic energy to be dissipated at impact could provide the means for defining the maximum impact velocity a capsule design can withstand. The requirements for this type of analysis are the ability to predict what portion of the total kinetic energy must be absorbed by capsule material deformation (as opposed to target deformation, rebound, etc.), the amount of capsule material which can be involved in deformation without a failure, and the high strain rate energy absorbing capability of the material.

An analysis of the distribution of impact energy and an evaluation, based on the performance of impact capsules A-3a, A-5a, and A-7a, of the high strain rate energy absorbing capability of the T-111 material has been made. These data could be used, in conjunction with total capsule weight, to predict theoretical maximum impact velocities for capsule survival. A more realistic maximum velocity for survival requires the correlation of the amount of capsule material involved in deformation prior to failure. This correlation would be dependent not only on capsule geometry but on impact velocity, angle, and deformation made. This correlation has not been attempted under the current program.

The energy absorbed by deformation of a pound of material is strongly dependent on the impact velocity. A factor, K, has been defined which is the ratio of this energy absorbed per pound dynamically to the energy under the normal stress-strain curve. Therefore,

$$K = \frac{E_{Dynamic}}{E_{Static}}$$

If K can be defined as a unique function of velocity for a given material and configuration, then prediction of the dynamic energy absorbing capability will be possible. The following paragraphs present the method for calculating the K factor, including the distribution of impact energies, and present the K factor for the three example impacts.

The procedure for evaluation of the K factor is as follows.

1) Energy-Absorption Capacity of Material

A measure of the energy absorption capacity of a material is afforded by its stress-strain curve. The static strain energy to fracture may be approximated as follows

$$E_s = \frac{1}{2}(\sigma_y + \sigma_u)\frac{\epsilon_u}{12\rho} \text{ (ft-lb/lb)} \qquad \ldots(1)$$

where

σ_y = the yield strength

σ_u = the ultimate strength

ϵ_u = elongation in percentage

ρ = density (lb/in.^{3})

2) Velocity of compressive wave or velocity of sound

$$C_c = \sqrt{E/\rho} \text{ (ft/sec)} \qquad \ldots(2)$$

where E is the modulus of elasticity.

3) Time Duration of Impact

$$\tau = \frac{2L}{C_c} \text{ (sec)} \qquad \ldots(3)$$

where L is the length of capsule.

4) Acoustic Impedance of Material

$$\rho C = \frac{\rho \times 144 \times 12}{32.2 \times 144} C = \frac{\rho 12}{32.2} C \text{ (psi/fps)}$$

5) Interface Pressure

For impact of a capsule with impedance $\rho_c C_c$ on the target media with impedance $\rho_t C_t$, the interface pressure expressed is

$$p = \frac{\rho_t C_t V}{1 + \frac{\rho_t C_t}{\rho_c C_c}} \text{ (psi)} \qquad \ldots(5)$$

6) Energy Dissipated in the Compressive Wave in the Target

$$E_{target} = \frac{2}{3} A \frac{\sigma^2}{E_t} \tau C_t \qquad \ldots(6)$$

where factor 2/3 is for the compressive stress distribution in the target, A is the contact area during impact, σ is the compressive stress in the target which can be equal to the interface pressure, and E_t is modulus of elasticity of the target media.

7) Energy dissipated in the compressive wave in the cylindrical capsule

$$E_{capsule} = \frac{2}{3} A \frac{\sigma^2}{E_c} \tau C_c \qquad \ldots(7)$$

For a hemispherical shell $E_{capsule}$ is reduced to

$$E_{capsule} = \frac{2}{3} \times \frac{2}{3} A \frac{\sigma^2}{E_c} \tau C_c \qquad \ldots(7)'$$

8) Total Kinetic Energy

$$K.E. = \frac{1}{2} \frac{W_c}{g} (V^2 - V_R^2) \qquad \ldots(8)$$

where

V = the impact velocity

V_R = the rebound velocity

For a cylindrical filled with powder material, the rebound velocity is very small.

9) Energy Dissipated in the Crater Volume

$$Q = \alpha \frac{\text{Vol} \times E_t}{1000 \times 12} = \alpha 540 \text{ Vol} \quad \text{(ft-lb)} \qquad \ldots(9)$$

where

Vol = the volume of the crater in in.^{3}

E_t = the modulus of elasticity of the target

α = reduction for low impact velocity

10) The energy absorbed by the deformed portion of the capsule

$$E_{\text{deformed}} = (8) - (6) - (7)' - (9) \qquad \ldots(10)$$

11) K Factor

$$K = \frac{E_{\text{deformed}}}{\text{Wt}_{\text{deformed}} \times E_s} \qquad \ldots(11)$$

where $\text{Wt}_{\text{deformed}}$ is the weight of deformed portion of the capsule.

When the capsule impacts onto the target in an oblique position, the total kinetic energy, $\frac{1}{2}MV^2$ is transformed into translational kinetic energy and rotational kinetic energy. The transitional kinetic energy at the impact end is reduced to

$$\left\{1 - \left[\frac{\sin \varphi}{\frac{1}{\sqrt{3}} + \sqrt{3}\sin^2 \varphi}\right]^2\right\} \frac{1}{2} MV^2 \qquad \ldots(12)$$

where φ is oblique angle with the axis perpendicular to the impact surface.

Using the properties for T-111 in Figure 36 and Table 2, the distribution of impact energies and K factors for capsules A-3a, A-5a, and A-7a were calculated. These data are shown in Table 3.

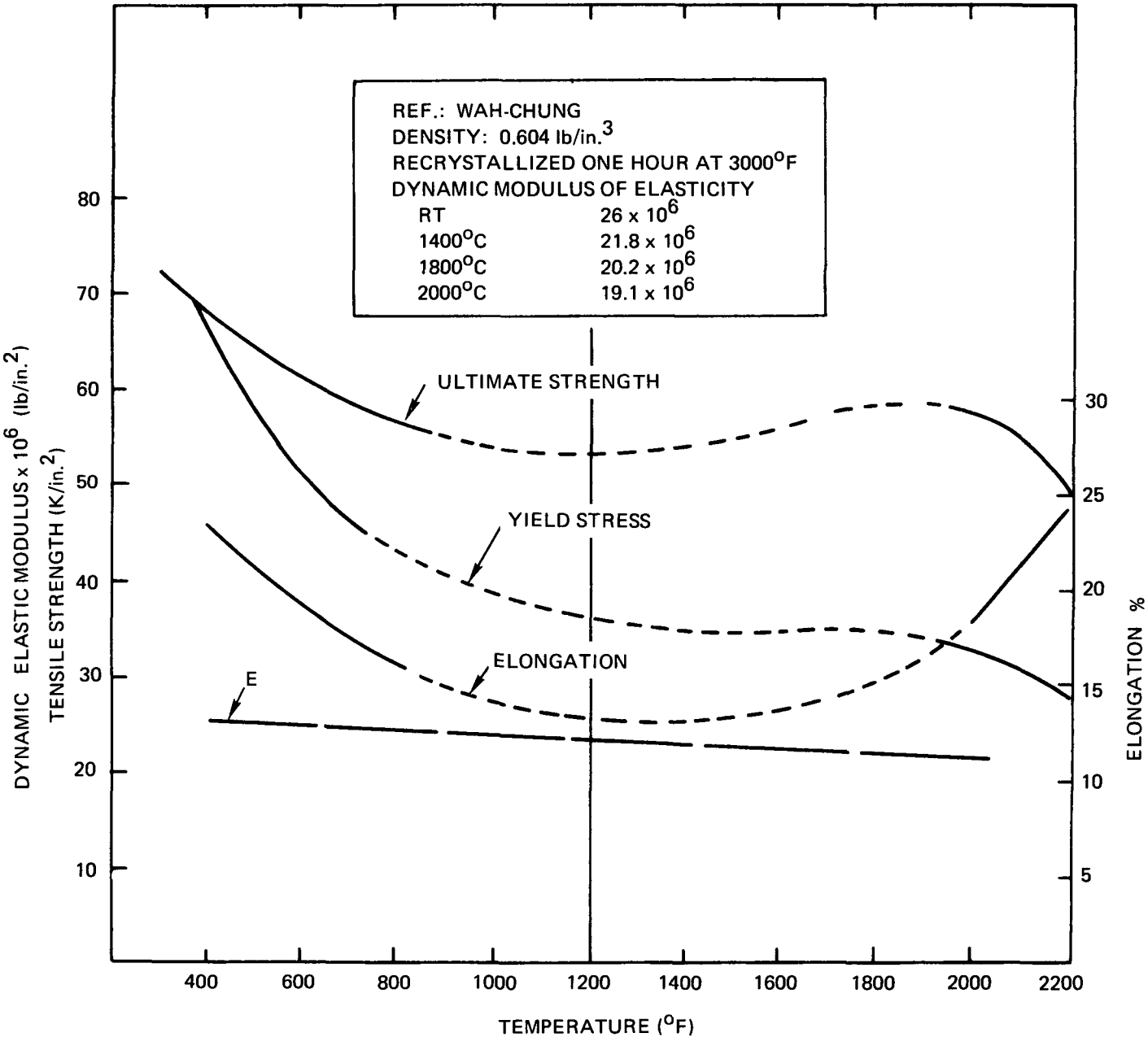

Figure 36. Properties of T-111

TABLE 2

PROPERTIES OF MATERIALS

Material	Temperature (°F)	σ_y ($K/in.^2$)	σ_u ($K/in.^2$)	ϵ_u (%)	E (10^6/psi)	ρ ($lb/in.^3$)	E_s (ft-lb/lb)	Velocity of Sound C (fps)	Impedance ρC (psi/fps)	Interface Pressure (psi)
T-111	1200	37	54	12	24	0.604	750	10,000	2,260	410 V
T-111	2000	36	59	18	22	0.604	1170	9,600	2,160	405 V
Granite Target	Room		40	0.6	6.5	0.102	100	13,000	500	

TABLE 3

IMPACT ENERGY DISTRIBUTION

Capsule S/N	Impact Velocity (fps)	Angle φ	Temperature (°F)	Diameter (in.)	Thickness, t (in.)	R/t Ratio	Weight (lb)	Area, πR^2 ($in.^2$)	Weight Per Impact Area (psi)	Cross-Section Area, πDt ($in.^2$)	$2\pi R_m^2 t$ (lb)	Deformed Cylindrical Shell	Total Deformed Weight (lb)
A-3a	260	0	1200	1.676	0.127	6.5	4.7	2.2	2.13	0.60	0.288	0.5	0.474
A-5a	240	0	1200	1.624	0.100	7.6	4.0	2.06	1.93	0.55	0.221	0.7	0.493
A-7a	346	0	1200	1.728	0.127	6.6	5.2	2.32	2.15	0.63	0.291	1.00	0.691

Capsule S/N	Total K.E. (ft-lb)	Static Energy E_s (ft-lb/lb)	Impact Duration, τ (sec)	Energy Dissipated in Target, E_t (ft-lb)	Energy Dissipated in Capsule, E_c (ft-lb)	Rebound Energy	Energy Dissipated in Target and Capsule (ft-lb)	Net K.E. (ft-lb)	$E_s \times Wt_{def.}$	K
A-3a	4940	750	1.26×10^{-4}	554	150	0	708	4132	356	11.6
A-5a	3600	750	1.26×10^{-4}	442	118	0	560	3040	370	8.2
A-7a	9700	750	1.26×10^{-4}	1055	285	0	1340	8360	520	16

PAGE BLANK

VI. CONCLUSIONS

The LRHSC impact test program has demonstrated that the reference materials, T-111 and Ta-10W, have sufficient ductility to survive terminal velocity impact and that the reference design capsule, with microspheres, will survive impacts of from 350 to 400 ft/sec.

Capsules which were impacted at angles between 45° and 20° from end on appeared to have incurred less severe deformation than capsules impacted at angles of less than 20°. This is a result of some energy being transferred to rotational motion and secondary impact. It is concluded that an end on impact is the most severe of those angles tested for this design, with the powder or microsphere fuel form.

The reference capsule's mode of failure, when impacted end on, is due to the formation of convolutions limiting the distribution of deformation to the cylindrical section, thus inhibiting the capsule's ability to dissipate absorbed energy. The result is a shear failure in the area between the impact surface and the first convolution. It is felt that this will indeed be the primary impact failure mode for capsules using a powder or microsphere fuel form.

REFERENCES

1. M. Marko, "Impact Tester Design and Analysis," AI-65-190, Vol. 7, December 1966

2. J. S. Williams, P. B. Ferry, "T-111 Pressure Vessel Development and Fabrication," AI-AEC-12712, Topical Report No. 4, July 25, 1968